Purdue University

Steel Bridge Research, Inspection, Training, and Engineering (S-BRITE) Center

Final Report - April 2018

Fatigue life improvement of welded girders with ultrasonic impact treatment

Jonathan F. Hui,
STV, Inc., jonathan.hui@stvinc.com
(Formerly of Purdue University)

Jason B. Lloyd,
Purdue University, lloyd1@purdue.edu

Robert J. Connor,
Purdue University, rconnor@purdue.edu

Table of Contents

LIST OF FIGURES

LIST OF TABLES

ABSTRACT

The fatigue life of welded connections can be improved by a variety of post-weld treatment methods. One of the most effective methods is ultrasonic impact treatment (UIT). This technology may be applied during shop fabrication, but the greatest benefit comes from field retrofitting applications.

Tensile cyclic stress ranges drive fatigue crack initiation and growth at the weld toe. This is made worse by tensile residual stresses at the weld toe that can reach the yield strength of the base metal resulting from differential cooling of the weld metal during fabrication. This concentration of tensile residual stress can have the effect of fully tensile cyclic stress ranges even in stress reversal zones of the bridge. UIT induces yield-strength level compressive residual stresses by cold forming the material at the weld toe.

Prior research has demonstrated the effectiveness of 27 kHz UIT systems for improving the fatigue life of welded bridge girders (Fisher and Roy, 2003). The AASHTO LRFD Bridge Construction Specification Commentary C11.9.1 suggests, but does not explicitly require, the use of 27 kHz systems. The existing language can be interpreted as a prohibition on other UIT systems.

This report explores the effectiveness of a 20 kHz UIT system applied to transverse stiffener and cover plate termination welds. In this study, fourteen full-scale girders with welded attachments were subjected to constant amplitude fatigue loading. The test matrix considered variables of stress range and minimum stress. Testing has shown that the 20 kHz UIT system provided equivalent effect to the 27 kHz UIT system. The treatment of the transverse stiffener welds improved the performance from Category C' to at least Category B. The performance of the cover plate termination welds improved from Category E' to at least Category C. The results demonstrated 20 kHz UIT as a viable option for enhancing the fatigue performance of welded bridge girders. This finding will expand the alternatives available to bridge owners seeking solutions for extending the life of their aging steel bridge inventory.

CHAPTER 1. INTRODUCTION

1.1 Project Overview

This purpose of this report is to document research completed at Purdue University Bowen Laboratory in partnership with SONATS SAS and its affiliates. This work was completed between May 2016 and February 2018. Due to unforeseeable mechanical faults, research completion was delayed. All tasks within the scope were ultimately completed within the initial budget. Findings were consistent with initial hypothesis.

The objective of the research was to demonstrate the effectiveness of 20 kHz ultrasonic impact treatment in fatigue retrofit of welded bridge girders. Fourteen, full-scale fatigue tests were conducted. Test results established equivalence of this technology and 27 kHz ultrasonic impact treatment, a proven fatigue retrofit technique. The new findings from this research are proposed for inclusion in the AASHTO LRFD Bridge Construction Specifications. The proposed code revisions make clear that 20 kHz ultrasonic impact treatment is a viable option for improving fatigue resistance of welded bridge structures. The proposed code revisions and supporting data were presented to AASHTO Subcommittee on Bridges and Structures in February 2018. Voting on the proposed revisions is set to take place later in 2018.

1.2 Project Team

1.2.1 *Robert J. Connor, Ph.D.*

Dr. Robert Connor is a Professor of Civil Engineering at Purdue University and Director of the Center for Aging Infrastructure.

1.2.2 *Jason B. Lloyd, P.E.*

Jason Lloyd is a Research Engineer at Bowen Laboratory and is a civil engineering doctoral candidate studying with Dr. Connor.

1.2.3 *Jonathan Hui, EIT*

Jonathan Hui was a civil engineering graduate student studying with Dr. Connor. Jonathan now works for STV, Inc., as a bridge design engineer in the rail transportation sector.

1.3 Fatigue Damage in Steel Bridges

Fatigue cracking is an essential consideration for the design and operation of steel bridges. Without intervention, cracks may propagate to an extent which causes the structure to fail. Fatigue cracks develop as the structure accumulates damage from recurring service level loads. This is known as load-induced fatigue. Fatigue cracks are initiated and propagated by tensile stresses induced by external loads.

Load-induced fatigue could occur in any part of a structure, but welded attachments are especially susceptible to this type of damage. The stress ranges induced in bridge girders by typical

vehicular loads is small, usually 5 ksi or less. Welds experience high magnitudes of tensile stress nonetheless and thus exhibit worse fatigue resistance than the base metal. Stresses are elevated at welds for multiple reasons.

The presence of the welded attachment introduces an abrupt change in the structural member's cross section. That discontinuity disturbs the stress field and induces a stress concentration at the weld toe. Additional stress concentrations can occur at flaws in the weld.

Welding induces tensile residual stresses that accelerate crack growth at weld toes. After fabrication, the weld loses heat and contracts. While the weld is molten, it contracts freely. The weld's exposed outer surface cools more rapidly its interior volume. Due to that temperature gradient, the outer surface solidifies first while the interior volume continues to contract. However, the solidified outer surface is restrained against that contraction by the adjacent steel. This figurative tug-of-war induces considerable tensile stress at the weld toes. Those stresses are locked into that location.

Many years of research on the fatigue behavior of steel bridges has culminated in the modern fatigue design provisions seen in the AASHTO LRFD Specifications. Recently constructed steel bridges offer excellent fatigue resistance due to the use of superior detailing. However, the nation's bridge inventory still includes numerous bridges designed prior to the current standards. Poor connection detailing often makes these older structures more susceptible to fatigue cracking. A common, problematic practice was the use of welded, partial-length cover plates to supplement the flexural strength of rolled beams. The stress concentration at the cover plate termination causes this detail to experience fatigue cracking under small stress ranges. Despite their shortcomings, many older, steel bridges will remain in service for the foreseeable future. It is not economically feasible to replace all those structures with ones designed to current specifications. This highlights the importance of developing viable retrofit solutions for improving fatigue resistance or reversing the effects of fatigue damage.

1.4 Overview of Fatigue Design Philosophy

Fatigue crack growth is driven by stresses at the weld toe. Determination of these localized hotspot stresses is an unwieldy and time-consuming task. To simplify the design process, current fatigue design provisions are based on the use of nominal stress analysis. This approach allows designers to take advantage of established closed form solutions based on the mechanics of materials. Once the nominal stress range has been calculated, the fatigue life of a connection can be read from the S-N diagram corresponding to its detail category.

The nominal stress design approach is founded upon extensive fatigue testing on a variety of welded attachment types. That research showed that the fatigue strength and fatigue life are linearly related when plotted on a log-log plot. Researchers observed that certain types of welded attachments exhibited similar fatigue resistance. These attachment types were grouped into detail categories, each with a characteristic design curve and constant amplitude fatigue limit. The design curve represents a lower bound on the range of fatigue resistances observed for the attachments belonging to that detail category. Conventionally, the design curve is placed two standard deviations below the mean life curve. This formulation ensures that the design fatigue resistance is achieved in almost all cases.

1.5 Ultrasonic Impact Treatment

There are a variety of established methods for improving the fatigue resistance of welded connections. Many retrofit techniques focus on altering the weld's exterior to induce more favorable stress conditions. These retrofits are commonly called surface treatments. Ultrasonic Impact Treatment (UIT)—also known as ultrasonic needle peening (UNP)—belongs to the family of surface treatments. Other types of surface treatments include grinding, air hammer peening and gas tungsten arc re-melting.

Of the many surface treatments, air hammer peening (AHP) is most closely related to UIT. AHP is applied using a pneumatically-driven hammer. The hammer features a chisel-like tip that impacts the weld toe. The surface is repeatedly struck by the hammer to develop a rounded, groove along the length of the weld toe. That permanent deformation is accompanied by compressive residual stresses. The undesirable tensile residual stresses left over from the weld fabrication are thus eliminated. UIT is based on the same physical process and produces a similar treatment appearance, albeit with a more sophisticated tool.

UIT offers many advantages over AHP. Although its outcomes are comparable to that of AHP, UIT makes use of electronic controls to greatly improve its ease of use. A certain amount of energy is required to induce permanent deformation in the weld toe. AHP delivers that energy via high amplitude, low frequency impacts. This causes a great deal of vibration and noise. In contrast, UIT uses ultrasonic waves to create low amplitude, high frequency impacts. The ultrasonic excitation frequency commonly ranges from 20 kHz up to 55 kHz, depending on the equipment manufacturer. Regardless of the frequency, UIT offers considerable reduction in vibration and noise relative to AHP. This reduction facilitates precise treatment application and a better working environment. The less aggressive impacts associated with UIT also help reduce the likelihood of damaging the material during treatment. There are minor tradeoffs related to UIT. Unlike AHP which is performed with generic tools, UIT is typically a proprietary system. This could potentially limit availability or increase cost.

1.6 Current AASHTO Specifications

Specifications regarding the use of UIT on bridge structures are published in the AASHTO LRFD Bridge Construction Specifications (Second Edition, 2008 Interim Revisions), Sections 11.9.1-3. Like the AASHTO LRFD Specifications, the document is structured with side-by-side code and commentary. Notably, the code is quite sparse at present and these sections are dominated by commentary on the background and usage of UIT.

Section 11.9.1 has no published code requirements and only provides commentary. This section's commentary introduces UIT and references supporting research completed at Lehigh University (Roy & Fisher, 2003).

A summary of the process is given along with a step-by-step description. The commentary discusses tool placement and handling, treatment speeds, pin diameters, and methods of identifying proper application. Section C11.9.1.4 calls for the use of 3-millimeter diameter pins wherever possible. The commentary states that smaller diameter pins are preferable since they are thought to provide more effective treatment. This section provides—as an example—some typical specifications of a 27-kHz ultrasonic impact treatment system. The provided specifications are for illustrative purposes only and may vary depending on the tool being used. There is no language that bars the use of frequencies

besides 27 kHz. The commentary section concludes with recommendations regarding the detrimental effects of heat treatment or high dead load on treated details.

Section 11.9.2 provides requirements on the ultrasonic impact treatment procedure. Requirements and limitations include a maximum base metal yield strength, maximum acceptable flaw sizes before treatment, placement of the treated area, and inspection metrics.

Section 11.9.3 prohibits welding and heat treatments after a detail has been treated. These procedures should not be used following UIT since they will relieve the compressive residual stresses that are the primary objective of UIT.

1.7 Current Practice

UIT is a relatively recent addition to the library of steel bridge fatigue retrofit techniques. As such there are not many published design specifications regarding its use in the bridge industry. Searches of published specifications from state departments of transportation yielded few specifications on UIT. This search located publications from only five states: Delaware, Indiana, Virginia, Texas, and New York.

The Delaware publication *DOT 2015 Bridge Design Manual: 109.9.3.4 Fatigue Evaluation and Repair* suggests UIT as an optional treatment to be used along with other fatigue retrofits of cover plates and transverse stiffeners without fatigue cracks or with very shallow flaws. The document provides no recommendation regarding the UIT equipment type or operating frequency.

The Indiana publication *Standard Specifications 711.31: Peening Welds by Means of Ultrasonic Impact Treatment (2016)* offers general guidance on UIT but gives no recommendations on the equipment frequency.

The Virginia publication *DOT 2016 Specifications: 426.03.C Ultrasonic Impact Treatment* mandates the use of UIT equipment with an excitation frequency of 27 kHz or 36 kHz. The pairing of 27 kHz and 36 kHz appears in other states' publications with nearly identical phrasing. The source of that requirement is not clear.

Similarly, the Texas publication Special Specification *7084 Ultrasonic Impact Treatment, 2004* and the New York publication *586.30010016 Ultrasonic Impact Treatment on Cover Plate Transverse End Welds* both mandate the use of UIT equipment with an excitation frequency of 27 kHz or 36 kHz.

CHAPTER 2. LITERATURE REVIEW

2.1 Full Scale Girder Tests

Multiple studies on the fatigue performance of welded bridge girders have been conducted at Lehigh University by Fisher and others. Those studies have investigated the effect of various types of welded details and fatigue retrofits. The findings from those pioneering studies were central to the development of the AASHTO LRFD fatigue design provisions.

In recent years, research has been conducted on the effectiveness of ultrasonic impact treatment as a fatigue retrofit option. These studies have investigated the treatment's effect on transverse stiffeners and partial length cover plates on rolled beams and plate girders. The results have shown that this treatment produces comparable fatigue life improvement as other post-weld retrofits such as air hammer peening. First, three treated plate girders were tested in a pilot study (Takamori and Fisher, 2000). An additional 19 rolled beams and 8 plate girders were tested in a subsequent study. (Roy and Fisher, 2003). The test results consistently showed UIT to be an effective option for extending the fatigue life of welded connection details. The data from fatigue tests of full-scale girders are particularly valuable since the effect of confounding variables should be minimized.

2.1.1 *Fisher et al, 1969*

This objective of this research was to develop statistically-based fatigue design provisions. Prior to this study, there had been limited research on the fatigue resistance of welded girders. The research up to that point was inadequate for developing statistical relationships for predicting fatigue life. Shortcomings of those earlier studies included insufficient control on the girder design parameters and insufficient replication. This study was focused on cover plate and flange splice details in rolled beams and welded plate girders.

The experimental program comprised fatigue tests of 374 beam specimens. Of the 374 specimens, 204 had welded, partial-length cover plates, 86 had no welded attachments, and 84 had welded flange splices. The test beams were either W14 x 30 rolled beams or welded plate girders of comparable size. Specimens were fabricated with A36, A441, or A514 steel. The specimens were simply supported on a 10-foot span and loaded in four-point bending. The cover plated specimens featured partial-length cover plates of differing geometries. The variables under consideration were the cover plate thickness, cover plate width, girder type, and the use of multiple cover plates.

It was concluded that stress range was the predominant factor influencing fatigue life of welded details. The cover plated specimens were tested at stress ranges at or above 6 KSI. All the specimens failed eventually and the infinite life threshold could not be identified. The cover plate geometry was found to have little effect on the fatigue resistance except for one subset. Cover plates which were wider than the flange and did not have a transverse termination weld had notably worse fatigue resistance than all the other cover plated details. The minimum stress was found to be insignificant except for cover plates without a transverse termination weld. Specimens fabricated from different steel types did not show any meaningful difference in fatigue life. This data was used to refute the idea that fatigue resistance increased with the steel yield strength. Analysis of the test results revealed that the relationship between stress range and fatigue life could be modeled with a linear fit of the log-transformed data. It was found that the fatigue life was inversely proportional to the cube of the stress

range. Application of fracture mechanics principles provided further evidence that this was an appropriate manner of modeling fatigue life.

2.1.2 *Fisher, et al, 1974*

The purpose of this study was to further the initial research on welded attachments (Fisher, et al, 1969). This study investigated the fatigue resistance of transverse stiffeners and longitudinally loaded attachments. In total, 157 specimens were tested with a variety of attachment types. 29 specimens did not have any welded attachments and were tested to establish a benchmark on the fatigue resistance of ASTM A514 base metal. Plate girders with welded transverse stiffeners comprised 22 specimens. The remaining specimens were W14 x 30 rolled beams with either welded transverse stiffeners (47 specimens) or longitudinally loaded attachments on the flange (59 specimens). The W14 x 30 specimens were of identical design as those used in the initial cover plate research, with the only difference being the type of welded attachment. The attachment plates were 9/32-inch thick and had length of 2 inches, 4 inches, or 8 inches.

It was concluded that as the attachment length increased, then the fatigue resistance at the end of the attachment became comparable to that at the end of a cover plate. Conversely, very short attachments such as welded transverse stiffeners had better fatigue life, and it was recommended that the welded stiffeners be assigned to their own detail category to reflect their superior performance

2.1.3 *Fisher et al, 1977*

The purpose of this study was to identify the largest flaw that would remain stable in cold temperatures. This research was motivated by fractures in in-service structures and the introduction of high strength steel and thicker plates. This study comprised three phases. First, 24 girder specimens with varying attachment details and steel grade were fatigue tested and then fractured. The second and third phases consisted of fracture toughness measurements and fracture mechanics analysis of the test specimens. Six specimens were tested with welded partial-length cover plates. Two were ASTM A36, W36 x 260 rolled beams; two were ASTM A588, W36 x 230 rolled beams; and two were ASTM A514, 36-inch deep plate girders. The rolled beam specimens' cover plates had a cross section measuring 1 inch by 12 inches. The plate girder specimens' cover plates had a smaller cross section measuring 1 inch by 4 inches. The rolled beam flanges were 1.25 inches thick and the plate girder flanges were 1.5 inches thick. At the time, these cover plate termination details had been classified as Category E. However, none of the test details surpassed the Category E design life. It was concluded that Category E, which was based on the prior research on cover plated W14 x 30 rolled beams, was unconservative for predicting the fatigue life of large, cover plated girders. This research would spur the addition of the Category E' detail in subsequent AASHTO Specifications.

2.1.4 *Fisher, et al 1979*

The objective of this study was to investigate the effectiveness of peening and gas tungsten arc re-melting as fatigue retrofits. The study was motivated by fatigue damage identified on the Yellow Mill Pond Bridge. The bridge had significant fatigue cracks at several cover plate terminations. The extent of damage was unexpected since the bridge was only 13 years old at the time and the live load stress range in those structural members was equal to the Category E endurance limit.

To establish a benchmark for the behavior of large cover-plated girders, 16 specimens were tested under cyclic fatigue loading. All the specimens were fabricated from W36 x 230 rolled beams. The

specimens were simply supported on a 19-foot span and had an overall length of 20-feet. The cross section of each cover plate was 1.25-inches by 12-inches. The cover plates were attached using 0.5-inch fillet welds running along the length of the plate and across the end. The specimens were subjected to constant amplitude loading with a stress range of either 4-ksi or 8-ksi. These specimens consistently displayed fatigue resistance inferior to that of the small cover plated beams tested in the initial study (Fisher, et al, 1969). They exhibited comparable performance as the first group of large, cover-plated girders (Fisher, et al, 1977). It was recommended that a Category E' be introduced to account for the worse fatigue resistance of large cover-plated girders.

2.1.5 *Takamori & Fisher, 2000*

This study evaluated several approaches for improving the fatigue life of welded bridge girders. The research comprised of three phases, the first two of which are relevant here. First, girders with repaired fatigue cracks were tested to measure their remaining fatigue life. Second, a small number of girders were tested to explore the use of ultrasonic impact treatment as an alternative retrofit for bridge girders. Prior research on ultrasonic impact treatment had shown its effectiveness on small scale specimens. This study aimed to extend those findings to full-scale bridge girders. Third, HPS girders were tested to determine the effectiveness of using under-matched welds as a means of improving weld quality.

To investigate the remaining fatigue life of repaired girders, fatigue tests were conducted on girders removed from the decommissioned Interstate 95 Yellow Mill Pond Bridge. These girders were cover plated W36 rolled beams of various weights. The steel type was ASTM A242. Constructed between 1956 and 1957, the structure was not designed according to modern fatigue provisions. Currently, the cover plate details would be classified as Category E'. The welded, partial-length cover plates performed poorly and developed fatigue cracks after two decades of service. The fatigue damaged girders were repaired in the field in 1976, using either gas tungsten arc (GTA) re-melting or air hammer peening (AHP). After the 1976 repair, no more fatigue damage developed and the girders performed satisfactorily through the retirement of the bridge.

The GTA retrofit eliminates the fatigue crack by melting the weld metal and neighboring base metal. As the metal solidifies, the weld metal and base metal become fused as one. GTA is also thought to eliminate impurities of the original weld.

Previous research showed that the GTA method produced retrofits with better performance under high minimum stress compared with air hammer peening. However, air hammer peening was found to be easier to use in the field, especially in tight spaces.

Six girders were removed from the Yellow Mill Pond Bridge for fatigue testing. All the girders were cover plated W36 x 230 rolled beams originating from the same bridge span. Each girder was cut down to a length of 17.5 feet for laboratory testing. Four of these girders had been retrofitted with AHP and the other 2 had been retrofitted with GTA instead. The specimens were subjected to constant amplitude fatigue loading with nominal stress range of 10 KSI at the cover plate termination. Each specimen was tested until fatigue cracks propagated through its tension flange.

All four of the girders repaired with AHP and one of the girders repaired with GTA surpassed the Category C design life. The second girder repaired with GTA survived past only the Category D design life. This was attributed to inadequate application of the GTA retrofit. The original crack was not fully eliminated by the repair and new fatigue damage initiated from that flaw. All the repaired welds failed due to fatigue cracks initiating at the weld root and propagating through the weld throat. The weld toes

remained undamaged. The alteration of the failure mode is indicative of the effectiveness of the repair. The study concludes that the AHP and GTA repairs were successful in removing the fatigue damage and restoring the girders' fatigue life.

In the second phase of this study, fatigue tests were performed on plate girders treated with UIT. Three, identical, 22-foot-long girders were fabricated for this test. The specimens included Category E' cover plate details and Category C' transverse stiffener details. The flanges and web were constructed using HPS-485W Grade 70 steel while the cover plates and stiffeners were constructed with ASTM A588 Grade 50 steel.

These girders had an overall depth of 36 inches, comparable to the W36 x 230 girders from the Yellow Mill Pond Bridge. One end of the girder had a 54-inch-long cover plate while the other end had a 37-inch-long cover plate. All the cover plates were 1 inch thick. Four pairs of transverse stiffeners were evenly spaced over an 8-foot length at the center of the girder.

There were 8 treated transverse stiffener details and 3 treated cover plate details. There were also 4 untreated transverse stiffener detail and 3 untreated cover plate details. The girders were loaded in four-point bending to produce a nominal flexural stress range of 16 KSI or 19 KSI at the transverse stiffener details and 8 KSI or 11 KSI at the cover plate terminations.

The details treated with UIT exhibited a comparable improvement as those treated with AHP or GTA. All the treated details survived through the end of testing except for one transverse stiffener detail. The fatigue tests were concluded when irreparable fatigue damage developed elsewhere along the tension flange. The transverse stiffener details all surpassed the Category B design life and the cover plate details all surpassed the Category C design life. The untreated details had fatigue life expected for their respective detail categories.

2.1.6 *Roy & Fisher, 2003*

This study follows up on the findings from Takamori and Fisher's pilot study on the effect of ultrasonic impact treatment. Building on that prior work, this study examines a broader scope of stress ranges and girder geometries. The residual stresses in the treated details was also measured.

All the test details were treated using a 27 kHz UIT system fitted with a 3-millimeter diameter pin. The needle oscillated with an amplitude in the range of 30 to 35 micrometers (approximately 0.001-inch).

The first group of specimens consisted of 18 W27 x 129 beams with welded transverse stiffeners and partial length cover plates. Each beam had a span length of 17 feet. The wide-flange beam was made of ASTM A588-97B Grade 50W steel. The attachment plates were made of ASTM A709-97B Grade 50W steel. Subsequently, an additional specimen was fabricated by splicing together the undamaged halves of two other specimens.

The specimen geometry was identical throughout except for the dimension of the fillet weld at the cover plate termination. Three alternatives were tested: no fillet weld, 0.5-inch fillet weld, and 1.0-inch fillet weld. The longitudinal fillet welds attaching the cover plate to the flange had equal leg lengths of 0.5 inches in all cases.

The specimens were simply supported on pin and roller bearings and subjected to four-point bending. The test matrix consisted variables of nominal stress range and minimum stress. Seven stress ranges were considered. Stress ranges varied from 7.5 KSI to 22 KSI at the cover plate terminations and

from 10 KSI to 29 KSI at the transverse stiffeners. Two levels of minimum stress were considered which were 1.5 KSI and 9 KSI at the cover plate terminations and 2 KSI and 12 KSI at the transverse stiffeners. The specimens were cycled until fatigue cracks propagated through the tension flange into the web.

None of the transverse stiffener details failed or developed observable cracks after testing. Damage at the cover plates prevented continuation of testing and the stiffener details were declared runouts. All of the transverse stiffener details had surpassed the Category B design life. Fourteen of the 18 specimens developed fatigue cracking at the cover plate termination welds. The cracks initiated from the weld toe in all but one case. Every treated cover plate detail considerably surpassed the Category E' design life. The amount of improvement varied depending on the size of the fillet weld at the cover plate termination. The treatment was found to be more effective when that weld was large relative to the plate thickness. When there was no fillet weld at the cover plate termination, the treatment improved performance only up as far as Category E. Cover plates with a treated, fillet weld at the termination improved up to Category D and as far as Category B in two cases. The treatment had the greatest effect on cover plates where the transverse fillet weld size was maximized. Cover plates with this detail improved to Category B at low stress ratios and Category C at high stress ratios.

The second group of specimens comprised 8 welded plate girders of 2 different designs. All 8 girders were fabricated using HPS 100W steel. The smaller design had a web which measured 30 inches by 0.75 inches and equal sized flanges which measured 7 inches by 1 inch. Six of the girders were fabricated according to this design. The remaining 2 girders had a taller web measuring 33.5 inches and a wider compression flange measuring 10 inches. Each girder had an overall length of 18 feet and was simply supported on a span of 17 feet. Pairs of transverse stiffeners were evenly spaced at three locations within the constant moment region. Each stiffener ran the full height of the web and was fillet welded to the web and both flanges. Similar stiffeners were also used at the bearing points and partial-depth stiffeners were used to stiffen the compression region of the web near concentrated forces. These specimens had no cover plates. The girders were tested under constant amplitude fatigue loading.

The test matrix included of 4 stress ranges and 5 minimum stresses. Of the 20 possible combinations, 6 were tested. Specimens HPS-1, HPS-2, and HPS-3 were tested with 9 KSI minimum stress and 19 KSI stress range. Specimen HPS-4 was tested with 20 KSI minimum stress and 20 KSI stress range. Specimen HPS-5 was tested with 20 KSI minimum stress and 16 KSI stress range. Specimen HPS-6 was tested with 14 KSI minimum stress and 14 KSI stress range. Specimens HPS-7 and HPS-8 were tested at 16 KSI minimum stress and 16 KSI stress range. Specimens HPS-3 and HPS-6 both survived past the design life of the web-to-flange weld. Since no fatigue damage was evident, these girders were tested again at higher loading. Specimen HPS-6 was retested at the loading of Specimen HPS-5. Specimen HPS-3 was tested at 24 KSI minimum stress and 16 KSI stress range.

On 4 of the plate girder specimens, the transverse stiffener details were not tested to failure. These tests were cut short by fatigue cracks propagating from the root of the web-to-flange weld. On 3 of the plate girder specimens, the transverse stiffeners developed fatigue cracks. The crack initiated from the weld root in 2 cases and from the weld toe in 1 case. The remaining plate girder specimens did not develop fatigue cracking at the stiffener details and were declared runouts. All the transverse stiffener details on the plate girder specimens surpassed the Category B design life.

Following the full-scale fatigue tests, specimens were analyzed to determine the treatment's effect on weld geometry and residual stresses. Fatigue-damaged weld details were removed from the specimens and the cracked regions were examined with a scanning electron microscope. It was observed that the treatment plastically deformed the steel at the weld toe to a depth of 0.2 mm.

A sample cover plate and flange assembly was fabricated for the study of residual stresses. The residual stresses induced by the treatment were measured using neutron diffraction. The analysis revealed that the compressive residual stresses were approximately equal to the steel's yield stress.

Based on this study, cover plate termination welds and transverse intermediate stiffener welds improved with ultrasonic impact treatment are given suggested fatigue categories. The cover plate termination welds are recommended to be classified as Category D under finite life loading and Category B under infinite life loading when the stress ratio is small—i.e. less than 0.1. When the stress ratio is up to 0.5, the same detail is recommended to be classified as Category E under finite life loading and Category C under infinite life loading. The transverse intermediate stiffeners are recommended to be classified as Category C' under finite life loading and Category B under finite life loading for stress ratios up to 0.5.

2.1.7 *Cheng, Yen, & Fisher, 2008*

The purpose of this study was to compare the effectiveness of three types of post-weld treatment: ultrasonic impact treatment (UIT), air hammer peening (AHP), and shot peening (SP). The treatments were applied to fillet welded stiffeners on a welded girder. The girder was fabricated with AL-6XN stainless steel and had a span of 10 feet. A total of 25 welds were treated: 10 by UIT, 12 by AHP, and 3 by SP. The UIT system used on these specimens operated at a frequency of 27 kHz. The UIT tool was fitted with four needles, each 3 mm in diameter. The girders were subjected to constant amplitude fatigue loading. The loading produced a nominal flexural stress of 8 KSI or 16 KSI at the treated details.

The test data indicated that the three treatments produced comparable fatigue life improvement. None of the specimens developed fatigue cracks at the weld toes. Fatigue tests were stopped after the treated details surpassed the Category B design life for stress range of 16 KSI. Two welds—one improved with UIT and one improved with SP—developed fatigue cracks from the weld root after exceeding the Category B design life. The specimens subjected to the 8 KSI stress range accumulated over 15 million cycles without any sign of fatigue damage. Those specimens were then tested again at the 16 KSI stress range. Despite having accumulated many cycles at the lower stress range, they exhibited no reduction in fatigue life. This suggests that the treatments eliminated fatigue damage at the lower stress range.

This study also measured the residual stresses induced by UIT and SP. Four steel plate specimens were fabricated for residual stress measurement by X-ray and neutron diffraction. The smallest plate measured 2 inches by 2 inches by 1 inch and the largest plate measured 6 inches by 6 inches by 0.5 inches. Three of the specimens were not welded and the fourth specimen had a T connection with 0.5-inch fillet welds. The test results showed that both UIT and SP induced compressive residual stresses comparable to the steel yield stress. UIT was found to have a further reaching effect, placing compressive residual stresses to a depth of 1.5 mm beneath the surface, whereas the influence of SP stopped at a depth of 0.8 mm.

2.2 Full Scale Tests of Non-Bridge Structural Components

2.2.1 *Palmatier, 2005*

This purpose of this study was to assess the use of ultrasonic impact treatment for enhancing the fatigue resistance of welded traffic signal structures. UIT was considered in usage as part of initial fabrication as well as a fatigue retrofit alternative.

An overview is provided of typical geometries of traffic signal masts in the state of Texas. These structures are mostly composed of steel tubing. The vertical tube (mast) and horizontal tube (arm) are fastened at a moment resisting connection that is shop welded and field bolted. At the moment connection, the open end of the horizontal tube is capped with a fillet welded base plate. From prior studies on traffic structures, it had been determined that this fillet weld detail is the typical point of failure.

A summary is provided of the UIT equipment used in the study. A water cooled, 27 kHz UIT system was used throughout. Several treatment heads were included, with varying number of peening needles of diameter ranging from 2 mm to 16 mm.

The arms were fabricated by shortening existing production sized tubes. Pairs of arms were connected at their base plates, forming a simply supported beam. This setup was chosen so that the vertical tube and moment connection would not need to be constructed in the laboratory. The simply supported beam was loaded with a concentrated load at mid-span—that is, at the fixed connection between the two arms—to induce moments equivalent to those in the real structure.

Constant amplitude, cyclic fatigue loads were applied with a 27-kip hydraulic actuator. Fatigue testing was carried out until the point of significant fatigue damage, namely a 5% loss of stiffness. Prior to testing, plastic molds were created of the fillet welds to create a record of the weld geometries.

2.3 Reduced Scale Specimen Tests

2.3.1 *Gunther, Kuhlmann, & Durr, 2005*

The researchers tested reduced scale specimens fabricated with S460M steel to model a typical transverse stiffener detail as used on welded plate girders. Untreated benchmark specimens were tested to failure to provide a reference with which to compare the performance of the treated specimens. Treated specimens were subjected to constant amplitude fatigue loads to expend the majority of the fatigue life prior to ultrasonic impact treatment. Ultrasonic impact treatment was found to be an effective retrofit, reversing the fatigue damage incurred up until when the treatment was applied. Ultrasonic impact treatment is effective in this regard if it is applied before significant fatigue cracks have developed in the welds. Most of the studies used X-ray or neutron diffraction measurements of residual stresses in treated specimens as a benchmark for the finite element models.

CHAPTER 3. EXPERIMENTAL METHODS

3.1 Introduction

The objective of this study was to investigate the fatigue resistance of welded attachments treated with 20 kHz ultrasonic impact treatment (UIT). Two types of welded attachments were considered, namely fillet welded, transverse, intermediate stiffeners and fillet welded, partial-length, cover plates. The effectiveness of 27 kHz UIT in improving these detail types had been established in prior research (Takamori & Fisher, 2000; Roy & Fisher, 2003). The results from this study were compared with the findings of the earlier research to demonstrate equivalence between treatments conducted with 20 kHz and 27 kHz UIT equipment.

3.2 Test Matrix

Specimens were tested under constant amplitude cyclic loading without load reversal. Stress range and minimum stress were the two variables considered in this experimental program. The test matrix as originally designed is shown in Table 3.1 and Table 3.2. The test matrix as ultimately applied is shown in Table 4.1. Prior research on beams with welded details had shown that stress range and detail type are the predominant factors affecting the fatigue life (Fisher et al, 1969). Subsequent research on welded details treated with UIT revealed that the minimum stress has a significant influence on the effectiveness of the treatment (Roy & Fisher, 2003). These two variables were investigated via 14 full-scale fatigue tests, 10 of which have been completed to date.

The stress ranges and minimums were selected to match a subset of those used in the previous UIT study (Roy & Fisher, 2003). The use of a similar test matrix and test specimens enabled easy comparison of the effects of 20 kHz and 27 kHz UIT systems.

This experimental program comprised 10 specimens treated with UIT and 4 specimens without treatment. The untreated specimens were tested to provide a benchmark against which the treated specimens' performance could be compared. Originally, the test matrix had included only two untreated specimens (S1 and S2). Later, it was considered desirable to provide additional benchmark data. Two untreated specimens (S7 and S8) were added to the test matrix, summing to the total of 14 specimens.

3.3 Failure Criterion

Defining failure is less straightforward with the fatigue limit state than other strength limit states. Determining whether fatigue damage has propagated to an extent constituting failure is a subjective judgment. The failure criterion used in this study has been chosen to match that used in the previous UIT research (Roy & Fisher, 2003). Failure is defined as the point when the fatigue cracks have propagated past the web-to-flange junction (K region). In some cases, the damaged detail was spliced before the crack propagated to the web, meaning that the detail did not proceed all the way to failure. Minimal error was introduced by this variation. Once the crack has extended the full width of the weld, few additional cycles are needed to propagate the crack through the remainder of the flange.

As defined, this failure criterion allows for more damage than would be considered acceptable on real bridges. It would be imprudent to wait until fatigue cracks have propagated through the flange

before taking action to repair the structure. However, use of this failure criterion does not exaggerate the detail's fatigue life to any meaningful degree. When cracking has been detected, the majority of the detail's fatigue life would already be expended. Observations during fatigue tests showed that the time at which cracks were first detected and the time at which cracks propagated to the failure criterion were separated by only a few thousand cycles. That number of cycles is small relative to the fatigue life and the scatter. Fish et al (2015) have estimated that up to 90% of the fatigue life is consumed by the nucleation phase of fatigue crack growth, supporting observations made during this research.

Fatigue data has a large amount of scatter, as much as an order of magnitude. Therefore, it is not feasible to continue each fatigue test to failure. At a certain point, the test is terminated even if no damage has yet occurred. Those results are reported as "runouts".

Prior research on 27 kHz UIT indicated that treated transverse stiffeners surpass the Category B design life and treated cover plates surpass the Category C design life (Roy & Fisher, 2003). The objective of this study was to determine if the same details treated with 20 kHz UIT would exhibit equivalent performance. Therefore, fatigue tests were continued—if not cut short by failures—until the transverse stiffener and cover plate details surpassed the Category B and C failure lives, respectively.

The AASHTO design life curves were based on the results of numerous full-scale fatigue tests of bridge girders with various types of welded attachments. Due to the considerable scatter in the fatigue life data, the design life curves were chosen to represent a lower bound. The design life curves were placed 2 standard deviations below their respective mean life curves. This means that 97.3% of details within a category are expected to meet or exceed the design life. Conversely, the failure life curves are placed 2 standard deviations above their respective mean life curves. The failure life represents the point when 97.3% of details within a category are expected to have failed. A detail that remains intact at the failure life has outperformed the overwhelming majority of details in that category. This provides strong evidence that the detail belongs to that category even though its unique fatigue life is not known.

The mean life can be determined from the design life using multipliers published in NCHRP Report 721 (Bowman et al, 2012). The failure life is calculated as twice the mean life less the design life.

3.4 Inspection Methods

Specimens were routinely inspected during fatigue tests. Fatigue crack initiation and growth was documented and the test apparatus were monitored to ensure they remained in good, working order. Inspection methods included visual observation, visual observation with the aid of a solvent, magnetic particle testing, and dye penetrant testing. The use of these techniques is summarized below.

3.4.1 *Visual Inspection*

This method was used in frequent, cursory checks of the specimens' conditions. A large flashlight and 10x magnifying glass were used to aid with the identification of damage. Small cracks were not readily identified with this method. However, it was well suited for tracking the growth of large cracks and for checking the overall integrity of the load frame and associated laboratory apparatus.

3.4.2 *Visual Inspection with Solvent*

This method was used routinely to identify small fatigue cracks which could not be observed with visual inspection alone. A degreasing solvent was sprayed onto the weld toes while the cyclic load

was applied. In regions without cracks, the solvent dispersed thinly along the surface and rapidly evaporated. Where a crack was present, a volume of the fluid would be drawn into the opening. The fluid is reflective and visibly pulses as the crack opens and closes under cyclic loading. A flashlight was used to increase the contrast between the fluid and the surrounding steel. Since this method depended on the specimen being in motion, it was not conducive to measuring crack lengths or documenting damage with photography.

3.4.3 *Magnetic Particle Testing*

Magnetic particle testing was regularly used to search for small cracks not observable by visual inspection. Testing was conducted using a magnetic contour probe manufactured by Parker. This inspection method could be used whether the specimen was in motion or at rest.

The probe is a handheld device powered by a 120 V AC power supply. There is an articulated, steel leg at each end of the device. The probe is positioned against the specimen such that one leg rests on either side of the test detail to be inspected. Pressing a trigger on the handle, activates a magnetic field between the legs. A small amount of red tinted, magnetic powder is sprinkled onto the area around the test detail. While the magnetic field is activated, a rubber bulb is used to direct puffs of air at the test detail, blowing away the excess powder. When a crack is present, the magnetic flux in the specimen becomes disturbed. This causes the powder to stick at the location of the crack. The powder remains at the crack even when the magnetic field is switched off. The crack is clearly highlighted in red and is readily measured or photographed.

3.4.4 *Dye Penetrant Testing*

This method was infrequently used as an alternative to magnetic particle testing. Cracks are identified with a dye that soaks into the crack and is subsequently brought to the surface. First, the test detail is wiped clean with a cleaning solvent and cotton rags. The dye penetrant is sprayed sparingly over the test detail and allowed to sit undisturbed for several minutes as the chemical penetrates any cracks. The excess dye penetrant is then wiped from the surface using a clean, cotton rag sprayed with a cleaning solvent. Once the surface had been thoroughly cleaned, the developer was sprayed onto the test detail. The developer extracts the dye penetrant contained in any cracks, which then appear red as the dye reaches the surface. This inspection method was typically used only after a fatigue test had finished. Considerable cleaning was necessary to remove the dye penetrant and developer before the detail could be inspected again. This made the dye penetrant method impractical for routine inspections which would take place several times throughout the day.

3.5 Specimen Design and Fabrication

Fourteen, cover-plated, rolled beams with transverse intermediate stiffeners were fabricated for full-scale fatigue testing. The overall specimen design is shown in Figure 3.3. The specimens were designed with welded connection details comparable to those on the specimens from the previous UIT study (Roy & Fisher, 2003).

All specimens were fabricated with ASTM A709 Grade 50 steel. The fabricator was also permitted to use ASTM A572 Grade 50 or ASTM A588 Grade 50 steels on the partial-depth stiffeners. The welded transverse stiffeners and partial-length cover plates were attached to the rolled beam with equal-leg fillet welds. The fabricator was required to be certified for AWS D1.5 fabrication and fabricate

the specimens according to AWS D1.5. This ensured that the weld quality would be representative of those on actual bridges. The partial-depth stiffeners were attached with fully-tensioned ASTM A325 bolts to achieve a slip-critical connection with the web.

The 14 specimens were fabricated in two groups by separate fabricators. The first group (Specimens 1 – 6) was fabricated by Kankakee Valley Steel. The second group (Specimens 7 – 14 and one unused specimen) was fabricated by Munster Steel. The specimen design received minor revisions for fabrication of the second group of specimens. However, the specimens within each group have the same design. Each specimen was built up from a 21-foot, W27 x 129 rolled beam. Symmetric, partial-length, cover plates were fillet welded to the lower flange. The fillet weld leg length was 1/2-inch. The cover plate cross section measured 7.5-inches by 1-inch. Stiffeners were fillet welded to the web and flanges. The fillet weld leg length was 5/16-inch. The interior corners of the stiffeners were chamfered to provide clearance at the web-to-flange junction. Bearing and full-depth intermediate stiffeners shared an identical design. Partial-depth stiffeners were provided to stiffen the web at the loading points.

3.6 Comparison of Specimen Designs

During the fatigue tests of Specimens 1 and 2, issues arose which motivated revisions in the design of Specimens 7 – 14.

Specimens 7 – 14 retained their original mill scale surface, whereas Specimens 1 – 6 had been blast cleaned to bare steel. The mill scale surface was preferred since it was more conducive to the identification of fatigue cracks. During fatigue testing, cracks were identified by spraying a solvent onto the weld toes while the load cycled. In regions without cracks, the solvent dispersed thinly along the surface and rapidly evaporated. Where a crack was present, a volume of the fluid would be drawn into the opening. The fluid is reflective and visibly pulses as the crack opens and closes under cyclic loading. The effectiveness of this method depends on the visual contrast between the solvent and the surrounding steel. Mill scale's dark color and low reflectivity are helpful in this regard. In contrast, blast cleaned steel's reflective, light gray surface made it more difficult to identify cracks. The roughened surface also caused solvent to pool in regions without cracks. The pooled solvent increased reflectivity and further reduced the visual contrast at cracks.

The cover plates on Specimens 7 – 14 were 49 inches long from the center of the support whereas those on Specimens 1—6 were only 47.5 inches long.

When initially delivered, Specimens 1 – 6 were found to have undercuts and other weld flaws that violated the requirements of AWS D1.5. The welds were repaired by the fabricator according to AWS D1.5 allowances and then accepted. The repaired welds appeared to offer equivalent fatigue resistance as the welds which had not needed repair.

The partial-depth stiffeners of Specimens 1 – 6 were fillet welded to the top flange in addition to being bolted to the web. The stiffener-to-flange fillet welds were omitted in Specimens 7 – 14 to prevent fatigue cracking. The concentrated force from the hydraulic actuators initiated fatigue cracking from the fillet weld roots. In Specimen 1, those cracks propagated through the fillet weld and top flange before arresting in the web. Cracking initiating from the weld root is difficult to detect and cannot be remedied by surface treatments such as grinding or UIT. Since these fillet welds were redundant, they were simply omitted from Specimens 7 – 14. On Specimen 1, the fatigue cracks were left in place while the test was completed. Specimen 5 was retrofitted by removing the fillet welds from the partial-depth stiffeners.

On Specimens 1 – 6, the full-depth transverse stiffeners were dimensioned to be flush with the flange tip. Also, the stiffener-to-flange fillet welds wrapped around from one face of the stiffener to the opposite face. This meant that some of those wraparound welds lay on the vertical face of the flange. This was considered undesirable since it created another potential location for initiating a fatigue crack. Where this condition was observed, the wraparound weld was removed with a grinding wheel and the remaining weld toe was treated with UIT. On Specimens 7 – 14, the wraparound fillet weld was omitted. Furthermore, the stiffener width was revised so that it stopped 0.5-inch short of the flange edge.

The inner corners of the transverse stiffener plates are chamfered to provide clearance at the web-to-flange fillet (K region). The height of this chamfer was enlarged on Specimens 7 – 14. This alteration provided additional space for maneuvering the ultrasonic impact tool when treating the stiffener weld toes.

3.7 Specimen Nomenclature

Each specimen has 6 test details: 2 transverse stiffener pairs (4 details) and 2 cover plates. As depicted in the Figure 3.13, the 8 stiffener fillet welds on the lower flange are labeled “A” through “H”. The cover plate termination welds are labeled “J” and “K”. There is no weld “I” to prevent misreading as a specimen identification number. Welds outside the scope of the test matrix were not labelled and are referred to only by their position as the need arises.

3.8 Laboratory Apparatus

All specimens were tested at Purdue University’s Robert L. and Terry L. Bowen Laboratory for Large Scale Civil Engineering Research. Two load frames were used to allow for concurrent testing of two specimens. Most of the specimens were tested entirely within one load frame. In two cases (Specimens 3 and 9), testing was started on one load frame and completed on the other to accommodate hydraulic actuator repairs.

3.8.1 *Hydraulic Actuators*

Loads were applied by 220-kip (220,000 lb.) capacity hydraulic actuators manufactured by MTS. The actuators are driven by hydraulic oil pressurized to 3000-psi by electric pumps. The actuators are designed to attain their maximum load in either tension or compression. In the laboratory, the actuators are calibrated for and used only in compression. The operating frequency is constrained by the actuator servo valves and the flow rate of the hydraulic pumps. In practice, the actuators operated between 1.00 Hz and 1.75 Hz. Five such actuators were rotated through the two test frames to facilitate actuator repairs. The actuators featured two different clevis designs. Three actuators were fitted with ball-joint type clevis at both ends, while two actuators featured a uniaxial hinge clevis at their top end.

The specimens were tested under fatigue loading without stress reversal and the compression load was 10 kips or greater throughout the load cycle. Since some compressive load was always maintained, no mechanical connection between the actuator and specimen was necessary. As an additional precaution, the control program included a software interlock restricting the upward displacement of the actuators. This interlock ensured that the actuators remained in contact with the specimen when the test was paused and there was no applied load.

A 2-inch by 16-inch by 24-inch plate was bolted to the rotating clevis at the bottom of each actuator. That plate distributed the load applied to the top flange of the specimen. A pair of smaller, 1.5-inch thick plates were bolted to the bottom of the large plate. These plates were used to keep the actuator centered over the specimen. Small angles clamped to the specimen top flange on either side of the large plate prevented the actuator from moving along the length of the specimen. Fatigue loading and cycle counting was controlled using the MTS Station Manager software package.

A varying number of fill plates were bolted to the bottom of the actuator. In this way, the wearing region on the actuator piston could be varied, thereby extending the life of that part.

3.8.2 *Load Frame Setup*

Specimens were simply supported on pin and roller bearings spaced at 20 feet on center. This span length was chosen to accommodate the spacing of anchor points in the laboratory strong floor and the minimum distance between the dual, overhead cranes. The typical specimen setup is depicted in Figure 3.1 and Figure 3.3. For clarity, bracing components have been omitted from those illustrations.

Each bearing comprised three components: a top plate, a cylindrical rod, and a bottom plate. The components were all 16 inches long. The diameter of the rod was 2.5 inches. On the roller bearing, the top and bottom plates were 1.5 inches thick and were milled to provide a smooth, flat surface upon which the rod rolled. The pin bearing was similarly constructed except that the plates were 2 inches thick and had been machined with a shallow groove which retained the rod. The grooves were lubricated with heavy bearing grease to reduce friction between the components. The bottom plate of each bearing assembly was bolted to bearing blocks made of stiffened, wide flange sections. The purpose of the bearing blocks was to elevate the specimen to be within the stroke of the hydraulic actuator. The bearing blocks rested on a leveling bed of gypsum cement atop concrete reaction blocks. The concrete reaction blocks are placed on a leveling bed of gypsum cement and anchored to the laboratory's strong floor with 1.25-inch diameter post-tensioning bars.

Each specimen's top flange was braced to prevent lateral instability. At each end of the specimen, heavy steel angles were bolted together to form a frame attached to the concrete reaction block. The frame prevented the flange from displacing laterally. The unbraced length between these braces was approximately 18 feet. Supplemental bracing was provided to secure the top flange at the loading points. Steel bars were used to attach each actuator's bottom plate to the flanges of the load frame columns. These bars act in tension to prevent excess lateral deflection. The supplemental bracing was designed only to engage in the event of significant lateral deflections. Their purpose is to provide an additional margin of safety against instability. During normal conditions, the supplemental bracing system carries no load. The bar can move freely throughout the specimens' normal range of motion. This design allowed the full effort of the actuators to be directed to the specimen and protected the load frame columns from cyclic, lateral loading.

The supplemental bracing was constructed with 0.5-inch by 2.5-inch steel bars. Each bar was fabricated with a 1-1/16-inch diameter, short-slotted hole at one end. The opposite end had a 1-1/16-inch diameter, standard hole. At each attachment point, the bar was sandwiched between Teflon plate washers to reduce wear from steel-on-steel contact. The bars are loosely attached to the column and actuator with 1-inch diameter ASTM A325 bolts. The nuts were only finger tight as not to restrain the rotational freedom of the bar. During fatigue testing, the continuous motion of the bar would tend to loosen the nuts. To prevent the nuts from backing out, double nuts or thread locking compound were used.

In each load frame, the actuators are spaced at a nominal distance of 8 feet on center. The actual spacing could vary 1 to 2 inches depending on the accuracy with which the actuator was attached to the frame. The load frame holds the hydraulic actuator in place over the beam and carries the applied load to the strong floor. The load frame consists of two moment frames constructed from W14 x 132 columns and W36 x 160 beams. The frame is braced along the by L 6 x 6 x ½ angles running diagonally from the columns to the laboratory strong floor.

Steel shims were provided as necessary between the bottom flange and bearing plates and between the top flange and the actuator clevis plate. The shims assisted in leveling the specimens and achieving a symmetric distribution of stresses across the flange.

3.8.3 *Alternate Load Frame Configuration*

Specimen 5 fatigue cycling was conducted using an alternate configuration of the load frame. The alternate specimen setup is depicted in Figure 3.2 and Figure 3.4. For clarity, bracing components have been omitted from those illustrations. The load frame was reconfigured to use only the north actuator to facilitate continuation of testing while the south actuator was overhauled. The concrete reaction blocks were repositioned to be symmetric with respect to the north actuator. The bearing blocks were removed and the pin and roller bearings were attached directly to the reaction blocks.

A spreader beam was placed between the actuator and specimen so that the load would be applied at the same points as in the original load frame configuration. The spreader beam consisted of a W18 x 130 beam. This beam was simply supported on the top flange of the beam specimen. A pin bearing was placed on the top flange over the specimen's north load point. A roller bearing was placed on the top flange over the specimen's south load point.

The actuator clevis was bolted to the spreader beam at its midpoint. Supplemental bracing bars were provided at mid-span for both the specimen and spreader beams. Small angles were clamped to the top flange of the specimen to keep the spreader beam laterally aligned.

3.8.4 *Additional Alterations*

As the experimental program progressed, the stability bracing design was gradually revised to improve access and strength. After fatigue testing of Specimen 5 concluded, the end bracing was altered to simplify specimen installation and removal. A threaded bar which had connected the two sides of the end bracing was removed. The two sides were moved apart so that the bracing no longer contacted the specimen flange edges directly. A plate was clamped to the specimen's top flange to fill the distance between the specimen and end bracing. The motivation of this design was to facilitate more efficient installation and removal of specimens. By separating the two halves of the end bracing, specimens could be craned through the bracing. Previously, the bracing had to be disassembled to provide access for the crane.

Beginning with Specimen 9, the end bracing was installed with tighter tolerances. Previously, there were small gaps between the flange and bracing to reduce frictional wear. Those gaps were eliminated to enhance the beams' stability against lateral torsional buckling under higher loadings.

3.8.5 *Ultrasonic Impact Treatment*

3.8.5.1 Equipment

Ultrasonic impact treatment (UIT) was carried out with the proprietary STRESSONIC system produced by SONATS. The system consists of a handheld UIT tool connected by an umbilical to the central control unit.

The central control unit contains the electronics which generate 20-kHz ultrasonic waves. That electrical signal is transmitted through the umbilical to the handheld unit where a piezoelectric emitter drives the peening needle. According to the manufacturer's specifications, the excitation signal cycles at 20 kHz ± 400 Hz and the needle oscillates with an amplitude of 0.002-inches. That amplitude was recommended for treating steel components.

The handheld tool may be fitted with different heads which accommodate different quantities and types of peening needles. A calibration attachment for the handheld unit is used to verify that the machine is operating at the correct amplitude. The peening needle is a consumable component and is replaced periodically as it is worn down by the impact forces.

3.8.5.2 Treatment Procedure

The treatment was applied by laboratory personnel qualified to operate the UIT equipment. Operators received training led by engineers from Empowering Technologies, a subsidiary of SONATS. Training comprised classroom instruction, as well as practical application.

To achieve the optimal effect from UIT, specimens were supported so that the treatment areas were under self-weight dead load stresses. Depending on space availability, the specimens were treated while in the load frame or supported on timber cribbing.

All specimens were treated using the same UIT equipment. The handheld tool was fitted with a single, 3-mm diameter peening needle. This is the needle diameter recommended by AASHTO LRFD Bridge Construction Specifications

Peening needles are available in different profiles for use with different surface geometries. Two different types of needles were used to treat these specimens. Most weld toes were treated using a needle with a bullet-shaped tip. A flat-tipped needle was used when the surface at the weld toe was relatively flat. The needle was regularly replaced as the tip was worn.

Effective treatment requires that the peening needle be properly oriented with respect to the treated surface. The handheld UIT tool was positioned so that the needle is perpendicular to the weld toe. Firm pressure was applied to the tool to maintain contact between the needle and the weld toe. This was especially important when using the tool in the overhead position.

The peening needle was advanced along the weld toe at a rate of approximately 0.5-inch per second. Treatment proceeded more slowly in regions where the weld toe changed directions. Reduced speed allowed the operator to verify that the peening needle was following the path of the weld toe. Care was taken to keep the tool moving. Excess pitting could result from the peening needle remaining too long in one location. This is especially important at the beginning or end of a treatment pass. To make sure that the weld toe is thoroughly treated, several passes are required. To help with the development of a uniform, grooved surface at the weld toe, the UIT tool was pivoted about longitudinal axis of the weld.

Properly treated areas have the distinctive appearance of a smooth, shiny groove running along the weld toe. The appearance of various details before and after treatment is depicted in Figure 3.7, Figure 3.8, Figure 3.9, and Figure 3.10. The treated areas were inspected visually with a flashlight and magnifying glass. The inspection verifies that the treatment follows the weld toe geometry. On certain details, the weld toe was not readily distinguishable. In these instances, the treatment area was expanded to include more of the base metal to ensure that the weld toe would be included. To supplement the visual inspection, the treated surfaces were probed with a welding rod. The welding rod is run with firm pressure along the groove developed by the UIT. In this way, the inspector may feel for any bumps indicative of untreated or poorly treated regions. At corners of the welds, care was taken to ensure that the treatment surface smoothly followed the weld toe without leaving any sharp edges.

Fatigue cracking is expected to occur first at weld toes that lie perpendicular to the primary stress (e.g. cover plate termination weld). Treatment was extended to adjacent sections of weld even if those welds were parallel to the primary stress. Per recommendations by the device manufacturer, treatment was also applied to any weld toes within 6 to 8 inches away from each test detail. A schematic of the treated regions surrounding each test detail are presented in Figure 3.5 and Figure 3.6.

The transverse stiffener fillet welds were treated along the length of the weld toe connecting to the tension flange. A length of the weld toe connecting to the beam was also treated. Following Specimen 9, the weld toes connecting to the compression flange were also treated as a precautionary measure.

3.9 Repair and Retrofit Procedures

3.9.1 *Typical Crack Arrest Hole Installation*

As described previously in Section 3.3, failure was defined as the point when fatigue cracks had propagated past the web-to-flange junction into the web. Upon failure, the fatigue test was paused and load was released from the girder. If further fatigue testing was required at other details on that specimen, then the failed detail was repaired to allow loading to resume. In general, the objective of the repair was to stop crack propagation and restore the compromised section.

First, the crack tip was located using magnetic particle testing or dye penetrant testing. These non-destructive testing techniques allowed the crack tip to be identified more reliably than by visual inspection alone. The crack tip and the surrounding region of the web were cored out using a magnetic drill press fitted with an annular cutter. The center of the hole was placed slightly ahead of the crack tip to ensure that the hole would capture the crack tip.

Crack tips on Specimens 2 and 4 were removed using a 2-inch diameter cutter. The hole was left open. This retrofit offered less fatigue resistance than desired. New fatigue cracks tended to initiate on the side of the hole opposite the original crack. Thus, this approach was abandoned after Specimen 4. The failure of a 2-inch diameter crack arrest hole and the subsequent repair is depicted in Figure 3.14. Subsequent specimens were retrofitted using 1-1/16-inch diameter holes fitted with a fully-tensioned, 1-inch diameter ASTM A325 bolt. This retrofit offered two main benefits. The bolted hole offered greater fatigue resistance than the open hole. Also, the smaller diameter cutter was easier to maneuver into tight spaces.

Both faces of the web were polished to a mirror finish near the crack arrest hole. Polishing helped to remove stress concentrations that could initiate additional fatigue cracks. The surfaces were

polished with an electric angle grinder fitted with 80-grit and 120-grit flap grinding discs. The inside surface of the hole was similarly polished to a mirror finish with an electric die grinder fitted with a 120-grit flap wheel. A 1/16-inch chamfer was applied to the sharp edges of the hole using the same flap wheel. After drilling and grinding were completed, the hole was wiped clean and visually inspected for burrs or other flaws. Magnetic particle testing was used to locate the arrested crack on the side of the hole, thereby confirming that the crack tip had been eliminated. A 1-inch diameter, ASTM A325 bolt was installed in the hole. There was no preference as to which side of the web the bolt head was placed. The bolt was snug tightened by with wrenches and then tensioned using an electric turn-of-the-nut wrench.

3.9.2 *Typical Flange Splice Installation*

With the crack successfully arrested, the next step was to install splice plates to substitute the flange section lost to cracking. At failure, the fatigue crack typically had propagated across the entire width and thickness of the flange. If the crack had not propagated through the entire flange, the crack tip within the flange was left in place. No crack arrest hole was required since the crack could propagate only as far as the flange tip. Saving the small, intact portion of the flange was not worthwhile, since the flange splice could carry all the stresses on its own.

The flange splice consisted of 1 outer plate and 2 inner plates. The outer plate was fitted below the flange and the inner plates were fitted above the flange on either side of the web. When the splice was installed at a cover plate termination, a 1-inch thick filler plate was placed between the outer plate and the portion of the flange without a cover plate. The splice centered lengthwise about the cracked flange section. The splice plates were sized rather conservatively since they were fabricated from existing materials at the laboratory. The splice length depended on the quantity of fasteners required for the applied load. When the fatigue crack initiated from a transverse intermediate stiffener weld toe, the bottommost 3 inches of the stiffener plate was removed to provide adequate clearance for the inner splice plates.

All mating surfaces were cleaned with a degreasing solvent to enhance friction. Initially, coarse sand was sprinkled between the plates, as this was thought to increase friction. The sand induced the opposite of the desired effect and was abandoned.

Whenever possible, the splice plates were fastened using heavy-duty, 6-inch C clamps, in lieu of bolts. Clamps helped eliminate the time-intensive task of drilling holes. A sufficient number of clamps was used to produce a slip-critical connection. The required number of clamps was estimated by assuming a clamping force of 27 kips and coefficient of static friction of 0.3. The assumed force was based on literature from the clamp manufacturer. The coefficient of static friction was based on the values published in the AISC Specifications. Each clamp was tightened using a socket wrench with a 2-foot pipe attached to the handle to lengthen the moment arm. The threaded spindle of each clamp was liberally coated with a spray-on white lithium grease to reduce friction and ease tightening.

Specimens with very high maximum stress were repaired with bolted splices instead since it became impractical to furnish the required number of clamps. These splices were fastened with 1-inch diameter, ASTM A325 bolts. The bolts were installed at 3-inch spacing along the length of the splice.

3.9.3 *Specimen 5 Partial-Depth Stiffener Weld Removal*

Shortly after the beginning of fatigue testing, fatigue cracks were identified on Specimen 5 at the fillet welds attaching the partial-depth stiffener to the compression flange. To prevent the possibility

of these cracks propagating through the compression flange as observed on Specimen 1, that detail was retrofitted.

Initial attempts to remove the crack with a flapper wheel grinder proved ineffective. Surface grinding confirmed suspicions that the cracks had propagated from the root. It was then decided to remove the fillet welds entirely. Each of the four stiffener angles were cut with an oxy-acetylene torch along a horizontal line 1/4 inch below their fillet welds. The stiffeners were then unbolted from the web and removed.

The fillet welds and remaining portion of the stiffener angles were ground flush to the inner surface of the compression flange with a grinding wheel. The surface was then polished smooth with a 120-grit flap wheel grinder. The ground surface was inspected with magnetic particle testing to ascertain that no cracks remained. The stiffener angles were then returned to their original positions and reattached with the same 7/8-inch diameter ASTM A325 bolts. As a precautionary measure, large timber blocks were driven into place adjacent to each partial-depth stiffener to limit distortion of the flange. The retrofit was successful and maintained the integrity of the compression flange through the end of the test.

3.9.4 *Specimen 9 Bolted Web and Flange Splices*

During testing, fatigue cracks were identified on Specimen 9 at several locations along the compression flange. The compression flange was significantly cracked in multiple locations in the contact patch of the south hydraulic actuator. It was not obvious from where these cracks had initiated. Several cracks extended through the thickness of the flange and one propagated downwards 6.5 inches into the web, parallel to the partial-depth stiffener. Additional fatigue cracks had initiated from the weld toes at the top of two, full-depth, intermediate stiffeners. The damage at the stiffeners was less severe than that at the actuator contact patch. These fatigue cracks had propagated through the flange thickness to the centerline of the flange. In the vertical direction, the cracks propagated as far as the web-to-flange junction. The fatigue damage on Specimen 9 was repaired with bolted web and flange splices to enable continuation of testing.

A bolted moment splice was installed along the top flange to redirect the flange stresses around the damaged cross sections. The required splice length was a significant fraction of the specimen's total length. The splice was lengthened so that specimen stiffness would be symmetric about the mid-span. Maintaining symmetry was necessary for ensuring that fatigue testing could proceed at the same stress ranges as before the repair.

The topmost 3 inches of each full-depth, intermediate stiffener was removed to provide clearance for the interior flange splice plates. Those portions of the stiffeners were cut away with an oxy-acetylene torch. The stiffener-to-flange fillet welds and the remaining portion of the stiffener plates were ground flush to the flange surface. The northern pair of partial-depth stiffeners were unbolted from the web and their topmost 1-inch was cut off with a band saw. The shortened stiffeners were returned to the web and attached with the original 7/8-inch ASTM A325 bolts, where possible. Bolts that had been damaged during removal were replaced in kind. The southern pair of partial-depth stiffeners were removed to make room for a web shear splice. Once the stiffeners had been removed, the crack tip in the web was identified and removed following the procedure described previously. The web shear splice was bolted to the web through the existing set of holes from the partial-depth stiffeners and a new set of holes drilled on the other side of the crack. It was fastened with a mix of 7/8-inch and 1-inch diameter, fully tensioned, ASTM A325 bolts

The fatigue cracks had propagated from the stiffener weld toes as far as the web-to-flange junction. Given the proximity to the transverse stiffeners, it was not possible to drill a crack arrest hole since the stiffeners interfered with operation of the magnetic drill press. Instead, a 1 1/16-inch diameter hole was drilled in the web 3 inches from either side of the stiffener. A slot was cut between these holes with an oxy-acetylene torch. The air gap in the web would capture any cracks propagating downwards. To improve the fatigue performance, the edges of each drilled hole were ground smooth with a flapper wheel grinder to remove burrs and gouges. A cylindrical flap grinder was used to grind the interior face and chamfer each edge of crack arrest holes.

The flange splice plates were fabricated from ASTM A709-50W cover plates salvaged from a built-up girder. The cover plates were trimmed down from their original width of 14 inches to match the flange width of the W27 x 129 beam. The cover plates had a staggered hole pattern of 15/16-inch diameter holes. The rows were spaced 4 inches on center. The outer holes were geometrically incompatible with the 10-inch flange of the W27x129. New 1 1/16-inch diameter holes were drilled between existing holes. The outer plate's cross section measured 0.75-inches by 10-inches. The two inner plates each had cross section measuring 1-inch by 4-inches. The plates were proportioned so that the outer plate's area was approximately equal to that of the inner plates.

The flange splice was designed to maintain a slip critical connection. The plates were fastened with fully tensioned, 7/8-inch diameter ASTM A325 bolts. At four locations, 1-inch diameter, ASTM A325 bolts were used instead. Due to the availability of 1 1/16-inch annular cutters, oversized holes were used at several locations. Bolts in oversized holes were installed with hardened washers on both sides. All bolts were tensioned using the turn-of-the-nut method with an electric wrench.

3.10 Static Load Tests

A static load test was conducted on each specimen prior to fatigue testing. The purpose of the static load test was to confirm that the programmed loads would produce the intended minimum and maximum stresses at the test details. Static load tests were repeated after repairs to the specimens, hydraulic actuators, or load frame.

Four types of measurements are continually monitored during the static load test. The applied load from each hydraulic actuator is measured by a load cell placed in line with the actuator piston. The displacement of each actuator piston is measured by a linear variable differential transformer (LVDT) within the actuator body. The displacement reading from the LVDT is not equivalent to the girder deflection, since the piston extension represents the combination of both the girder and load frame deflections. The primary function of the LVDT measurement is to provide input to the software interlocks. If the displacement exceeds a predetermined value, the interlocks automatically shut off hydraulic pressure to the actuators. This safety feature minimizes the risk of damage should the specimen become unstable. The girder deflection is measured by string potentiometers attached to the bottom flange beneath each actuator. Strain was measured by strain gages attached to flange near each test detail. The data logger program converted strain measurements to stress readings with an assumed steel elastic modulus of 29000 KSI. The measurements from the load cells, string potentiometers, and strain gages were recorded at frequency of 5 Hz for the duration of the static test.

Load application during static load tests was controlled by computer program written within the MTS Station Manager software package. Once the instrumentation had been zeroed, the load was ramped up to the level corresponding to the minimum stress. The load was held constant for several seconds to provide time for any load fluctuations to attenuate. The load was then ramped up to the

level corresponding to the maximum stress and held constant for several seconds. Load was then smoothly reduced to zero. Stress and displacement readings were checked to see that they had returned to zero as well. Non-zero readings would be indicative of problems with the instrumentation. If problems occurred, the static test was stopped and started anew once the errors had been resolved. If the instrumentation was functioning properly, the loading cycle would be repeated two more times.

3.10.1 *Instrumentation*

Data was collected using a Campbell Scientific CR9000 data logger fitted with a pair of 9050 Analog Input cards. The data logger was controlled using the RTDAQ software package provided by Campbell Scientific. Data collection was active only during static load testing.

All specimens were instrumented with bondable strain gages manufactured by Tokyo Sokki Kenkyojo Limited. The gage length was 6 millimeters and the gage resistance was 350±1.5 Ω. The gauge factor was 2.11±1%. These specifications were provided by the manufacturer for 23 degrees Celsius and 50% relative humidity which closely corresponded with the conditions in the laboratory. The position of the strain gages on the specimens is illustrated in Figure 3.11 and Figure 3.12.

The bondable strain gages were glued to specially prepared surfaces on the specimen. At each strain gage location, mill scale was removed with an 80-grit flap wheel grinder. The surface was then polished to a mirror finish with a 200-grit and 400-grit belt sander. Reference lines were scribed into the ground surface to aid in the alignment of the strain gage. Any burrs created by the scribing process were removed with 400-grit sandpaper. The surface was cleaned with a degreasing solvent and cotton gauze.

The strain gages were attached to the specimen using a cyanoacrylate glue recommended by the strain gage supplier. The strain gage was held in position using clear, plastic tape while applying the glue. The strain gage was firmly pressed against the specimen for 1 minute to ensure that the entire surface of gage was firmly bonded. After the glue had cured for 20 minutes, the clear, plastic tape was removed. A polyurethane coating was then brushed over the gages to protect them from the environment. The strain gage wires were secured to the specimen with aluminum tape to keep them from being torn off inadvertently.

Each strain gage was manufactured with a length of cable. Those cables were trimmed within a few inches of each gage, and shielded cables were used to attach the gages to the data logger. Shielded cables were preferred since their grounded metallic wrapping helped reduce interference to the electrical signal from the gages. The strain gauge lead wires were connected to the wires of the shielded cables with either 3M Scotchlok UY Butt Connectors or WEGO Lever Nut Connectors.

CHAPTER 4. TEST RESULTS & DISCUSSION

4.1 Synopsis

Fatigue testing has been completed for 4 as-welded specimens and 10 treated specimens. The treatment proved to be highly effective at extending the fatigue life of Category C' transverse stiffener details and Category E' cover plate details. The treated details have exhibited fatigue resistance characteristic of Category B and Category C, respectively.

4.2 Analysis

The recorded fatigue life of the test details was compared with the calculated design, mean, and failure lives corresponding to that detail and stress range. Per AASHTO LRFD Bridge Design Specifications, untreated transverse stiffeners are classified as Category C' and untreated cover plate terminations are classified as Category E'. Prior research indicated that treated transverse stiffeners behaved according to Category B and treated cover plate terminations behaved according to Category C (Roy & Fisher, 2003). Therefore, the treated details were compared using fatigue life constants calculated from those categories.

Following standard design practice, the design fatigue life was calculated using the nominal flexural stress range at the test detail. The nominal flexural stress range was calculated using mechanics of materials equations and the recorded minimum and maximum loads from the static load tests. These calculated values are summarized in Table 4.1. The recorded loads were compared against the recorded strain and displacement data to verify that the specimens were behaving as expected. The recorded loads, strains, and displacements were consistent with one another and in agreement with values predicted by mechanics of material equations and finite element analysis.

The results of the fatigue tests are summarized in Table 4.2. Typical examples of fatigue damage are presented in Figure 4.1, Figure 4.2, and Figure 4.3.

The mean life was determined by factoring the calculated design life by the detail multipliers published in NCHRP Report 721 (Bowman, et al, 2012). The failure life was determined according to the relationship that $N_{failure} = 2N_{mean} - N_{design}$. The calculated design, mean, and failure life of each specimen is presented in Table 4.3.

4.3 As-welded Specimens

Specimens 1, 2, 7, and 8 were tested in the as-welded condition. The results from these specimens reflect the large degree of scatter associated with fatigue test data. Several test details exhibited fatigue resistance at the upper end of the expected ranges for their respective detail categories. Similar cases of highly fatigue resistant, as-welded beams have been reported in other research (Takamori & Fisher, 2000).

Some transverse stiffener details displayed fatigue resistance worse than the Category C' design life. Fatigue life data has very large magnitude of scatter and these results are not surprising.

The results of the four as-welded specimens reaffirm the classification of transverse stiffeners as Category C' and cover plate terminations as Category E'. The test results for the as-welded specimens are summarized in Table 4.2. The results are plotted with the AASHTO design curves in Figure 4.7 and Figure 4.8.

4.3.1 *Specimen 1*

Specimen 1 was tested with nominal stress ranges of 18.9-ksi at the transverse stiffeners and 13.7-ksi at the cover plate terminations. Fatigue testing concluded after 2.5 x 10^6 cycles. The test was declared a run-out after the number of cycles exceeded the Category C' failure life (2.1 x 10^6 cycles) at the transverse stiffener details. The cover plate details surpassed the Category E' failure life 425 x 10^3 cycles. At the conclusion of the test, no fatigue cracks were detected in any of the test details. However, fatigue cracks were detected elsewhere on the specimen. A crack initiated from the fillet weld attaching the partial-depth stiffener to the upper flange. That crack was not detected until it had propagated through the compression flange. Similar fatigue cracking at the partial-depth stiffener appeared on Specimen 5. Several fatigue cracks also developed at the fillet welds attaching the bearing stiffeners to the lower flange. These cracks appeared to have initiated at the weld root, propagated through the weld throat, and arrested at that extent. The fatigue cracking at the bearing stiffeners appeared on all subsequent specimens.

4.3.2 *Specimen 2*

Specimen 2 was tested with nominal stress ranges of 18-ksi at the transverse stiffeners and 13.1-ksi at the cover plate terminations. Fatigue testing concluded after 2.9 x 10^6 cycles. The test was stopped after the number of cycles exceeded the Category C' failure life (2.4 x 10^6 cycles) at the transverse stiffeners. No fatigue cracks were detected at the transverse stiffener details. Fatigue cracks developed at the end of each cover plate. In both cases, the fatigue crack initiated at the weld toe near the flange centerline. The fatigue cracks propagated through the flange within several thousand cycles after initiation. The south cover plate failed after 8.2 x 10^3 cycles. The fatigue damage at the south cover plate is depicted in Figure 4.2. The north cover plate failed after 1.1 x 10^6 cycles. The cover plates failed after the exceeding their Category E' failure life (490 x 10^3 cycles).

4.3.3 *Specimen 7*

Specimen 7 was tested with nominal stress ranges of 18-ksi at the transverse stiffeners and 13.5-ksi at the cover plate terminations. Fatigue testing concluded after 420 x 10^3 cycles. The test was stopped due to fatigue failure of the test details. In all failed test details, fatigue cracking initiated from the weld toes and then propagated through the lower flange. The south cover plate failed after 240 x 10^3 cycles. Its number of cycles at failure surpassed the Category E' design life (160 x 10^3 cycles) but was less than the Category E' mean life (300 x 10^3 cycles). The south cover plate's fatigue resistance is within the range expected for Category E' details. The north cover plate failed after 414 x 10^3 cycles. Its number of accumulated cycles at failure surpassed the Category E' mean life (300 x 10^3 cycles) but was less than the Category E' failure life (444 x 10^3 cycles). The south transverse stiffener detail failed after 420 x 10^3 cycles. The number of cycles at failure was less than the Category C' design life (750 x 10^3 cycles). The north transverse stiffener detail exhibited fatigue cracking after 420 x 10^3 cycles. The fatigue cracking at the north transverse stiffener had not propagated through the flange. This detail was not tested to failure since it was not practicable to repair the extensive fatigue damage at the other details. However,

given the considerable amount of cracking observed at that point, it is reasonable to conclude that the north transverse stiffener would have failed prior to the Category C' design life.

4.3.4 *Specimen 8*

Specimen 8 was tested with nominal stress ranges of 18-ksi at the transverse stiffeners and 13.5-ksi at the cover plate terminations. Fatigue testing concluded after 627 x 10^3 cycles. The test was stopped due to fatigue failure of the test details. At all the failed test details, fatigue cracking initiated from the weld toes and then propagated through the lower flange. The south cover plate exhibited considerable cracking after 414 x 10^3 cycles. The damaged detail was spliced before failing. However, given the amount of cracking at that point, it is reasonable to conclude that the failure was imminent. Its number of cycles at failure exceeded the Category E' mean life (300 x 10^3 cycles) but was less than the Category E' failure life (440 x 10^3 cycles). The north cover plate exhibited considerable cracking at 627 x 10^3 cycles. This detail was not tested to failure since it was not practicable to repair the extensive fatigue damage at the other details. Its number of cycles at termination of testing exceeded the Category E' failure life (440 x 10^3 cycles). Both the south and north transverse stiffener details failed after 627 x 10^3 cycles. Each of these details failed prior to the Category C' design life (754 x 10^3 cycles).

4.4 Treated Specimens

Testing has been completed for all of the 10 treated specimens. The results indicate that ultrasonic impact treatment is highly effective. All but one of the transverse stiffener details have exceeded the Category B failure life. The one exception has been the only transverse stiffener detail to have developed fatigue cracks so far. That detail failed shortly after reaching the Category B design life.

All but one of the cover plate details have surpassed the Category C failure life. One cover plate detail failed after surpassing the Category C mean life but prior to the failure life. Of the 20 cover plate details (one from each end of the 10 treated specimens), 12 cases resulted in fatigue crack initiation at the transverse weld root, three cases cracked at the treated toes, and five cases had no detectable cracks at the conclusion of testing. This points to the effectiveness of the weld toe treatment. A fatigue curve was fitted to the S-N data from these three cover plate failures. The fatigue curve slope was set at -3 to match the slopes of the AASHTO finite life curves. The curve was fit to the data with the least squares method. The detail constant, A, was calculated to be 11 x 10^9. The cover plate fatigue curve lies between the Category C mean and failure life curves. This is further evidence that the treated cover plates have performance equivalent to Category C details.

The test results of the treated specimens are presented in Table 4.2 and are plotted in Figure 4.4 and Figure 4.5. The fatigue curve fitted to the cover plate fatigue life is plotted in Figure 4.6 along with AASHTO design curves.

4.4.1 *Specimen 3*

Specimen 3 was tested with nominal stress ranges of 17.8-ksi at the transverse stiffeners and 12.9 ksi at the cover plate terminations. Fatigue testing concluded after 6.6 x 10^6 cycles. Testing was stopped after the number of accumulated cycles reached the Category C failure life at the cover plate details (6.6 x 10^6 cycles). No fatigue cracks were detected at any of the test details and the test was declared a runout. The transverse stiffener details survived past the Category B failure life. The

treatment had yielded considerable improvement in the fatigue performance. The test details have improved by at least one AASHTO categories.

4.4.2 *Specimen 4*

Specimen 4 was tested with nominal stress ranges of 18.1-ksi at the transverse stiffeners and 13.1-ksi at the cover plate terminations. Fatigue testing concluded after 6.2 x 10^6 cycles. Testing was stopped due to extensive propagation of fatigue cracks which rendered repair impracticable. The south transverse stiffener detail failed after accumulating 2.3 x 10^6 cycles. Fatigue cracks initiated from the fillet weld toe on the lower flange. The crack propagated across the flange and into the web within several thousand cycles. The south transverse stiffener detail failed after surpassing the Category B design life (2.0 x 10^6 cycles). The fatigue damage at the transverse stiffener is depicted in Figure 4.1. The damaged flange was spliced and testing resumed. The repair was ultimately unsuccessful. A fatigue crack initiated from an open crack arrest hole and propagated a considerable distance into the web. Fatigue cracks also initiated in the lower flange at accidental gouges left over from the repair procedure. At this point, the cover plate details were only several thousand cycles short of the Category C failure life (6.3 x 10^6 cycles). The extent of damage and proximity to the failure life informed the decision to stop the test. After testing both cover plate details remained intact and no cracks were detected at either detail. The north transverse stiffener detail remained intact after testing and no cracks were detected at that detail. The north transverse stiffener exceeded the Category B failure life (6.1 x 10^6 cycles).

This was the only specimen from the test matrix which exhibited a failure at a transverse stiffener detail. The failure is possibly the result of inadequate application of the ultrasonic impact treatment, however, this could not be confirmed. Subsequent specimens would have had higher quality treatment due to increased experience with using the treatment tool.

Except for the one transverse stiffener detail discussed above, Specimen 4 exhibited similar performance as Specimen 3 which was tested at comparable stresses. The treatment has yielded considerable improvement in the fatigue performance. The test details have improved by at least one AASHTO categories.

4.4.3 *Specimen 5*

Specimen 5 was tested with nominal stress ranges of 14-ksi at the transverse stiffeners and 10.2-ksi at the cover plate terminations. Fatigue testing concluded after 13.1 x 10^6 cycles. The test was declared a run-out. No cracks were detected at any of the test details. The cover plates were 200,000 cycles short of surpassing the Category C failure life (13.3 x 10^6 cycles).

Although none of the test details on Specimen 5 developed detectable fatigue cracks, fatigue cracks initiated at the fillet welds of the partial-depth stiffeners. The failure mode was identical to that observed on Specimen 1. As reported previously, the partial-depth stiffeners were retrofitted and no further cracking occurred in the upper flange.

4.4.4 *Specimen 6*

Specimen 6 was tested with nominal stress ranges of 14.1-ksi at the transverse stiffeners and 10.2-ksi at the cover plate terminations. Fatigue testing concluded after accumulating 13.0 x 10^6 cycles. The north cover plate detail failed after 11.8 x 10^6 cycles. Fatigue cracking initiated at the cover plate transverse weld root. The crack then propagated through the weld throat and across the lower flange. The treated weld toe remained intact and had no detectable cracks. At the time of failure, the north

cover plate detail had exceeded the Category C mean life (8.7 x 10^6 cycles), but had not surpassed the Category C failure life (13.3 x 10^6 cycles). The south cover plate detail remained intact through the conclusion of testing. It was 300,000 cycles short of the Category C failure life when testing was terminated. The transverse stiffener details remained intact through the conclusion of testing and no cracks were detected. These details survived past the Category B failure life (12.8 x 10^6 cycles) and were declared run-outs.

4.4.5 *Specimen 9*

Specimen 9 was tested with nominal stress ranges of 23.9-ksi at the transverse stiffeners and 17.9-ksi at the cover plate terminations. Testing was paused after 1.1 x 10^6 cycles to enable repair of fatigue damage in the upper flange. No cracks were detected in any of the test details at that point. Both cover plates developed weld root failures at 1.7 x 10^6 cycles. The fatigue damage at the south cover plate is depicted in Figure 4.3. The flanges were spliced and testing resumed. The cover plates had surpassed the Category C mean life (1.6 x 10^6 cycles), but not the Category C failure life (2.5 x 10^6 cycles). Fatigue testing concluded after 3.0 x 10^6 cycles. No fatigue cracks were detected along any of the transverse stiffener details. These details survived past the Category B failure life (3.0 x 10^6 cycles) and were declared run-outs.

4.4.6 *Specimen 10*

Specimen 10 was tested with nominal stress ranges of 24-ksi at the transverse stiffeners and 18-ksi at the cover plate terminations. Fatigue testing concluded after 2.4 x 10^6 cycles. Testing was stopped after extensive propagation of fatigue cracks in the upper flange and web. The north cover plate failed after 1.5 x 10^6 cycles. The failure was comparable to that of the Specimen 6 cover plate. Fatigue cracks initiated from the cover plate transverse weld root and propagated through the weld throat and across the lower flange. The damaged flange was spliced and fatigue testing continued. At the time of failure, the north cover plate had exceeded the Category C design life (750 x 10^3 cycles) was 100,000 cycles short of the Category C mean life (1.6 x 10^6 cycles). The south cover plate fared better and failed after 2.3 x 10^6 cycles. It also failed due to a fatigue crack initiating from the cover plate transverse weld root. At the time of failure, the south cover plate had approached the Category C failure life (2.5 x 10^6 cycles). At the termination of testing, the transverse stiffener details had survived past the Category B mean life (1.8 x 10^6 cycles) and were 200,000 cycles short of the Category B failure life (2.6 x 10^6 cycles).

4.4.7 *Specimen 11*

Specimen 11 was tested at nominal stress ranges of 18.7-ksi at the transverse stiffeners and 14-ksi at the cover plate terminations. Fatigue testing concluded after 5.7 x 10^6 cycles. Testing was stopped after the number of accumulated cycles surpassed the Category B failure life (5.5 x 10^6 cycles) at the transverse stiffener details. No cracks were detected at any of the test details. After testing, the cover plate details had survived past the Category C failure life (5.1 x 10^6 cycles).

4.4.8 *Specimen 12*

Specimen 12 was tested at nominal stress ranges of 19.2-ksi at the transverse stiffeners and 14.4-ksi at the cover plate terminations. After 1.26 x 10^6 cycles had elapsed, the south cover plate detail fractured. The damaged section was repaired with a bolted flange splice and testing resumed. After 2.58 x 10^6 cycles had elapsed, the north cover plate termination weld failed. The damaged section was repaired with a bolted flange splice and testing resumed. The fatigue test was terminated after 3.31 x

10^6 cycles, due to failure of the bolted flange splice at the failed north cover plate detail. The development of fatigue cracks at the bolted detail was unexpected since similar splices exhibited considerably higher fatigue resistance. A probable cause for the splice failure was incorrect installation of the splice bolts. It is hypothesized that the bolts were not tightened to their specified pretension. This condition would expose the drilled holes to high bearing stresses which accelerated fatigue crack initiation. At the end of the test, no fatigue cracks were detected at any of the transverse stiffener test details.

At termination of the fatigue test, the transverse stiffener details had surpassed the Category B design life (2 x 10^6 cycles) and were about 80,000 cycles short of the Category B mean life (3.38 x 10^6 cycles). The south cover plate termination detail failed only 250,000 cycles short of the Category C design life. Close examination of the failed weld toe suggests that the impact treatment performed by the research team on Specimen 12 south cover plate weld toe was less than complete. A few locations appeared to have a gap in treatment. Figure 4.3c shows a magnified image of a properly treated toe demonstrating the smooth, shiny appearance that results. Figure 4.3d & 4e provide a contrast to this where it can be seen that the treatment left areas of untreated or insufficiently treated weld toe where stress risers would likely reduce fatigue resistance. These figures are magnified photos of Specimen 12 south cover plate weld at locations which indicated fatigue initiation points. Following testing, the welded detail was removed from the specimen and examined. Several small fatigue cracks were observed to initiate and coalesce forming one larger fatigue crack. This type of fatigue crack growth is not uncommon, but nonetheless supports the observation of multiple locations of insufficient treatment. The areas of poor treatment would contribute to the reduced fatigue resistance, relative to the other tested details. This singular data has therefore been excluded from Figure 4.5. The research team is of the opinion that due to the inconsistent treatment of the weld toe this data point should not be included in the overall data set. It clearly does not represent the fatigue resistance that the remainder of the data clearly demonstrate is achieved when the weld toe is properly treated. The north cover plate termination detail failed after surpassing the Category C design life (1.5 x 10^6 cycles), but prior to surpassing the Category C mean life (3.09 x 10^6 cycles). These results are consistent with the hypothesis that treated transverse stiffener details perform as Category B and treated cover plate terminations perform as Category C.

4.4.9 *Specimen 13*

Specimen 13 was tested with a nominal stress range of 23 ksi at the transverse stiffener details and 18 ksi at the cover plate terminations details. A fatigue crack was detected at the north cover plate termination detail after 1.25 x 10^6 cycles had elapsed. The fatigue crack had initiated from the untreated transverse weld toe along the vertical plane of the cover plate. No fatigue cracks were observed at the treated transverse weld toe along the flange. At 1.41 x 10^6 cycles, similar cracking was observed on the south cover plate termination detail. The damaged sections were repaired with bolted flange splices and testing resumed. The initiation of fatigue cracks at the untreated toe is indicative of the treatment's effectiveness.

At 1.85 x 10^6 cycles, the fatigue test was stopped by the program interlocks. The test details were inspected and no damage was identified. The fatigue test was restarted, but was stopped by the program interlocks once more. The test was restarted a second time and after 10 cycles, the specimen fractured at its midspan. The fracture ran upwards to approximately half the web depth. The damaged section was inspected to investigate the cause of fracture. Observation suggests that fatigue cracking initiated in the base metal of the lower flange initiating at a rolling defect from the mill. This crack initiated away from the test details and had not been detected prior to the fracture. The fatigue cracks

appeared to have propagated to the web-to-flange junction before fracture occurred. It was not practical to repair the extent of damage incurred from the fracture and the fatigue test was concluded at this point. No fatigue damage was observed at any of the treated transverse stiffener details.

At termination of the fatigue test, the transverse stiffener details had surpassed the Category B design life (986 x 10^3 cycles) and were approaching the Category B mean life (1.97 x 10^6 cycles). At time of failure, the north cover plate termination detail had surpassed the Category C design life (754 x 10^3 cycles) and was approaching the Category C mean life (1.58 x 10^6 cycles). Similarly, the south cover plate termination detail failed after surpassing the Category C design life but prior to reaching the Category C mean life. These results are consistent with the hypothesis that treated transverse stiffener details perform as Category B and treated cover plate terminations perform as Category C.

4.4.10 *Specimen 14*

Specimen 14 was tested with a nominal stress range of 24 ksi at the transverse stiffener details and 19 ksi at the cover plate terminations details. A fatigue crack was observed along the transverse weld toe of the south cover plate after 1.50 x 10^6 cycles had elapsed. A bolted flange splice was installed at the damaged section and testing resumed. A fatigue crack was observed at the north cover plate termination at 1.88 x 10^6 cycles. At time of detection, the crack had propagated into the beam web. Due to the extent of the damage to the specimen, it was not feasible to perform repairs and fatigue testing was terminated at 1.88 x 10^6 cycles. No fatigue cracks were detected at any of the transverse stiffener details at the conclusion of testing.

At termination of testing, the transverse stiffener details had surpassed the Category B design life (1.74 x 10^6 cycles). Both cover plate termination details had surpassed the Category C design life (1.35 x 10^6 cycles) and were approaching the Category C failure life (2.05 x 10^6 cycles) at time of failure. These results are consistent with the hypothesis that treated transverse stiffener details perform as Category B and treated cover plate terminations perform as Category C.

CHAPTER 5. CONCLUSIONS & FUTURE WORK

5.1 Conclusions

Test results indicate that 20 kHz ultrasonic impact treatment (UIT) offers equivalent performance as 27 kHz UIT. The treatment substantially improves fatigue resistance of welded details.

The treatment effectiveness was investigated via fatigue tests of full-scale welded bridge girders. Two types of weld details were studied: fillet welded transverse stiffeners and fillet welded cover plate terminations. Treated transverse stiffener details surpass Category B design life and treated cover plate termination details surpass Category C design life.

The test results indicate that the treated stiffeners surpass Category B design life and the treated cover plate terminations surpass Category C design life. This shows that 20 kHz UIT is a viable retrofit option and has equivalent effect as 27 kHz UIT, which was the subject of prior research (Roy & Fisher, 2003). Treatment with 20 kHz UIT yields significant improvement in fatigue life and existing specifications should be updated to reflect this finding.

The objective of this study was to observe the effect of 20 kHz UIT on the fatigue resistance of welded details where toe cracking is the most likely type of cracking. Fourteen girder specimens were tested for this experiment. Weld details on ten of the specimens were treated with UIT. The remaining four specimens were tested in their as-welded condition. Each specimen was fabricated from W27 x 129 rolled beam with welded transverse stiffeners and partial length cover plates. In the as-welded condition, these details are classified as Category C' and E' respectively. The test matrix comprised two levels of minimum stress and three stress ranges. Ten treated specimens were tested along with four as-welded benchmark specimens. Prior research on 27 kHz UIT showed that treated transverse stiffener details surpassed Category B design life and treated cover plate termination details surpassed Category C design life. To show that 20 kHz and 27 kHz UIT offer equivalent improvement, the specimens were tested under constant magnitude fatigue loading until failure or upon exceeding the 97.5% failure life of their improved detail category.

All of the treated transverse stiffener details surpassed Category B design life. Fatigue cracks initiated at only one transverse stiffener detail. This detail developed fatigue cracks at the treated weld toe after surpassing Category B design life. No fatigue damage was detected at any of the other treated transverse stiffener details. These results show that 20 kHz UIT considerably improves fatigue resistance and is as effective as 27 kHz UIT.

Twelve cover plate termination details failed after developing fatigue cracks originating from the interior of the weld. Three cover plate termination details failed with fatigue cracks initiating at the treated toe, and five cover plate termination details had no detectable fatigue cracks at the conclusion of testing. The failures occurred after the details surpassed the Category C design life, at a minimum, and many after exceeding Category C mean life. The surviving details reached Category C failure life. On as-welded cover plate termination details, fatigue crack initiation is expected to take place at the weld toe. On the treated details, fatigue cracks most often initiated from the interior weld rood.

The findings from these fatigue tests are consistent with results from prior studies on the effect of 27 kHz UIT. This demonstrates the equivalence of the two treatments. It is recommended that AASHTO LRFD Bridge Construction Specifications Section C11.9.1 be amended to include reference to these findings showing the effectiveness of 20 kHz UIT. This reference will increase clarity and minimize

the misconception that UIT must be conducted with 27 kHz systems to be effective. It is also recommended that the example procedure from that section be updated to include operating parameters for 20 kHz UIT along with the existing values listed for 27 kHz UIT. These alterations will allow designers to specify the use of this beneficial technology more easily. Proposed changes to the AASHTO specifications can be found in Appendix I.

Numerous fatigue tests conducted in this study and in previous research has consistently shown the poor fatigue resistance of welded cover plates. These details are not commonly used anymore but remain on many in-service structures constructed prior to modern fatigue design provisions. The poor fatigue performance of these details makes them good candidates for fatigue retrofits. Post-weld surface treatments such as ultrasonic impact treatment have been shown to be an effective method for elevating fatigue resistance by introducing beneficial compressive residual stress at the weld toe.

TABLES

Table 3.1: Planned Test Matrix for Transverse Stiffener Details

S_{min} [KSI]	S_r [KSI]		
	14	**19**	**24**
2	S5	S1, S2, S3, S4, S7, S8	S9, S10
12	S6	S11, S12	S13, S14

Table 3.2: Planned Test Matrix for Cover Plate Termination Details

S_{min} [KSI]	S_r [KSI]		
	10.5	**14**	**18**
1.5	S5	S1, S2, S3, S4, S7, S8	S9, S10
9	S6	S11, S12	S13, S14

Table 4.1: Nominal Flexural Stress at Test Details

ID		Load		Nominal Flexural Stress											
				S = M c / I						S = ε E					
				Intermediate Stiffeners			Cover Plate			Intermediate Stiffeners			Cover Plate		
		P_{min}	P_{max}	S_{min}	S_{max}	S_r	S_{min}	S_{max}	S_r	S_{min}	S_{max}	S_r	S_{min}	S_{max}	S_r
#		kip	kip	ksi	ksi	ksi	ksi	ksi	ksi	ksi	ksi	ksi	ksi	ksi	ksi
1		10.4	108.7	2.0	20.9	**19**	1.5	15.6	**14**	2.0	21.0	**19**	1.6	16.6	**15**
2		10.1	104.2	1.9	20.0	**18**	1.5	15.0	**14**	2.0	19.6	**18**	1.5	15.5	**14**
3		10.0	102.7	1.9	19.7	**18**	1.4	14.8	**13**	2.0	19.8	**18**	1.6	15.8	**14**
4		10.0	104.2	1.9	20.0	**18**	1.4	15.0	**14**	2.0	19.3	**17**	1.5	15.3	**14**
5		10.0	83.0	1.9	15.9	**14**	1.4	11.9	**10**	1.9	15.4	**14**	1.4	12.2	**11**
6		61.6	135.2	11.8	25.9	**14**	8.8	19.4	**11**	11.5	25.2	**14**	9.2	20.0	**11**
7		10.0	104.0	1.9	20.0	**18**	1.4	14.9	**14**	1.8	19.8	**18**	1.6	17.7	**16**
8		10.0	104.0	1.9	20.0	**18**	1.4	14.9	**14**	1.8	20.1	**18**	1.6	17.7	**16**
9		10.5	135.0	2.0	25.9	**24**	1.5	19.4	**18**	2.0	25.2	**23**	1.6	20.8	**19**
10		10.5	135.5	2.0	26.0	**24**	1.5	19.5	**18**	2.2	25.8	**24**	1.6	21.2	**20**
11		62.4	160.0	12.0	30.7	**19**	9.0	23.0	**14**	12.2	31.0	**19**	9.9	24.8	**15**
12		62.0	162.0	11.9	31.1	**19**	8.9	23.3	**14**	11.7	30.1	**18**	9.8	25.0	**15**
13		62.7	187.7	12.0	36.0	**24**	9.0	27.0	**18**	11.3	34.4	**23**	9.0	28.5	**20**
14		62.6	187.7	12.0	36.0	**24**	9.0	27.0	**18**	11.3	34.8	**24**	9.2	29.2	**20**

Table 4.2a: Fatigue Test Results, Transverse Stiffener Details

Untreated Transverse Stiffeners

Specimen	Type	Detail	Position	S_r	$N_{Failure}$	$N_{End\ of\ Test}$
S1	CONTROL	TS	SOUTH	18.9		2.5E+6
S1	CONTROL	TS	NORTH	18.9		2.5E+6
S2	CONTROL	TS	SOUTH	18.0		2.9E+6
S2	CONTROL	TS	NORTH	18.0		2.9E+6
S7	CONTROL	TS	SOUTH	18.0	420E+3	
S7	CONTROL	TS	NORTH	18.0	420E+3	
S8	CONTROL	TS	SOUTH	18.0	627E+3	
S8	CONTROL	TS	NORTH	18.0	627E+3	

Treated Transverse Stiffeners

Specimen	Type	Detail	Position	S_r	$N_{Failure}$	$N_{End\ of\ Test}$
S3	UIT	TS	SOUTH	17.8		6.6E+6
S3	UIT	TS	NORTH	17.8		6.6E+6
S4	UIT	TS	SOUTH	18.1	2.3E+6	
S4	UIT	TS	NORTH	18.1		6.2E+6
S5	UIT	TS	SOUTH	14.0		13.1E+6
S5	UIT	TS	NORTH	14.0		13.1E+6
S6	UIT	TS	SOUTH	14.1		13.0E+6
S6	UIT	TS	NORTH	14.1		13.0E+6
S9	UIT	TS	SOUTH	23.9		2.9E+6
S9	UIT	TS	NORTH	23.9		2.9E+6
S10	UIT	TS	SOUTH	24.0		2.4E+6
S10	UIT	TS	NORTH	24.0		2.4E+6
S11	UIT	TS	SOUTH	18.7		5.7E+6
S11	UIT	TS	NORTH	18.7		5.7E+6
S12	UIT	TS	SOUTH	19.2		3.3E+6
S12	UIT	TS	NORTH	19.2		3.3E+6
S13	UIT	TS	SOUTH	23.0		1.9E+6
S13	UIT	TS	NORTH	23.0		1.9E+6
S14	UIT	TS	SOUTH	24.0		1.9E+6
S14	UIT	TS	NORTH	24.0		1.9E+6

Table 4.2b: Fatigue Test Results, Cover Plate Termination Details

Untreated Cover Plates

Specimen	Type	Detail	Position	S_r	$N_{Failure}$	$N_{End\ of\ Test}$
S1	CONTROL	CP	SOUTH	13.7		2.5E+6
S1	CONTROL	CP	NORTH	13.7		2.5E+6
S2	CONTROL	CP	SOUTH	13.1	817.8E+3	
S2	CONTROL	CP	NORTH	13.1	1.1E+6	
S7	CONTROL	CP	SOUTH	13.5	235E+3	
S7	CONTROL	CP	NORTH	13.5	414E+3	
S8	CONTROL	CP	SOUTH	13.5	627E+3	
S8	CONTROL	CP	NORTH	13.5	627E+3	

Treated Cover Plates

Specimen	Type	Detail	Position	S_r	$N_{Failure}$	$N_{End\ of\ Test}$
S3	UIT	CP	SOUTH	12.9		6.6E+6
S3	UIT	CP	NORTH	12.9		6.6E+6
S4	UIT	CP	SOUTH	13.1		6.2E+6
S4	UIT	CP	NORTH	13.1		6.2E+6
S5	UIT	CP	SOUTH	10.2		13.1E+6
S5	UIT	CP	NORTH	10.2		13.1E+6
S6	UIT	CP	SOUTH	10.2		13.0E+6
S6	UIT	CP	NORTH	10.2	11.8E+6	
S9	UIT	CP	SOUTH	17.9	1.7E+6	
S9	UIT	CP	NORTH	17.9	1.7E+6	
S10	UIT	CP	SOUTH	18.0	2.3E+6	
S10	UIT	CP	NORTH	18.0	1.5E+6	
S11	UIT	CP	SOUTH	14.0		5.7E+6
S11	UIT	CP	NORTH	14.0		5.7E+6
S12	UIT	CP	SOUTH	14.4	1.3E+6	
S12	UIT	CP	NORTH	14.4	2.6E+6	
S13	UIT	CP	SOUTH	18.0	1.4E+6	
S13	UIT	CP	NORTH	18.0	1.3E+6	
S14	UIT	CP	SOUTH	19.0	1.5E+6	
S14	UIT	CP	NORTH	19.0	1.9E+6	

Table 4.3: Calculated Design, Mean, and Failure Life

SPECIMEN	DETAIL	POSITION	CATEGORY	NOMINAL STRESS RANGE	DETAIL CATEGORY CONSTANT	DETAIL MULTIPLIER	$N_{SURVIVAL}$	N_{MEAN}	$N_{FAILURE}$
S1	TS	S	C'	18.9	4.4E+9	2.1	652E+3	1.4E+6	2.1E+6
	TS	N	C'	18.9	4.4E+9	2.1	652E+3	1.4E+6	2.1E+6
	CP	S	E'	13.7	390.0E+6	1.9	152E+3	288E+3	425E+3
	CP	N	E'	13.7	390.0E+6	1.9	152E+3	288E+3	425E+3
S2	TS	S	C'	18.0	4.4E+9	2.1	754E+3	1.6E+6	2.4E+6
	TS	N	C'	18.0	4.4E+9	2.1	754E+3	1.6E+6	2.4E+6
	CP	S	E'	13.1	390.0E+6	1.9	173E+3	330E+3	486E+3
	CP	N	E'	13.1	390.0E+6	1.9	173E+3	330E+3	486E+3
S3	TS	S	B	17.8	12.0E+9	2.0	2.1E+6	4.3E+6	6.4E+6
	TS	N	B	17.8	12.0E+9	2.0	2.1E+6	4.3E+6	6.4E+6
	CP	S	C	12.9	4.4E+9	2.1	2.0E+6	4.3E+6	6.6E+6
	CP	N	C	12.9	4.4E+9	2.1	2.0E+6	4.3E+6	6.6E+6
S4	TS	S	B	18.1	12.0E+9	2.0	2.0E+6	4.0E+6	6.1E+6
	TS	N	B	18.1	12.0E+9	2.0	2.0E+6	4.0E+6	6.1E+6
	CP	S	C	13.1	4.4E+9	2.1	2.0E+6	4.1E+6	6.3E+6
	CP	N	C	13.1	4.4E+9	2.1	2.0E+6	4.1E+6	6.3E+6
S5	TS	S	B	14.0	12.0E+9	2.0	4.4E+6	8.7E+6	13.1E+6
	TS	N	B	14.0	12.0E+9	2.0	4.4E+6	8.7E+6	13.1E+6
	CP	S	C	10.2	4.4E+9	2.1	4.1E+6	8.7E+6	13.3E+6
	CP	N	C	10.2	4.4E+9	2.1	4.1E+6	8.7E+6	13.3E+6
S6	TS	S	B	14.1	12.0E+9	2.0	4.3E+6	8.6E+6	12.8E+6
	TS	N	B	14.1	12.0E+9	2.0	4.3E+6	8.6E+6	12.8E+6
	CP	S	C	10.2	4.4E+9	2.1	4.1E+6	8.7E+6	13.3E+6
	CP	N	C	10.2	4.4E+9	2.1	4.1E+6	8.7E+6	13.3E+6
S7	TS	S	C'	18.0	4.4E+9	2.1	754E+3	1.6E+6	2.4E+6
	TS	N	C'	18.0	4.4E+9	2.1	754E+3	1.6E+6	2.4E+6
	CP	S	E'	13.5	390.0E+6	1.9	159E+3	301E+3	444E+3
	CP	N	E'	13.5	390.0E+6	1.9	159E+3	301E+3	444E+3
S8	TS	S	C'	18.0	4.4E+9	2.1	754E+3	1.6E+6	2.4E+6
	TS	N	C'	18.0	4.4E+9	2.1	754E+3	1.6E+6	2.4E+6
	CP	S	E'	13.5	390.0E+6	1.9	159E+3	301E+3	444E+3
	CP	N	E'	13.5	390.0E+6	1.9	159E+3	301E+3	444E+3
S9	TS	S	B	23.9	12.0E+9	2.0	879.0E+3	1.8E+6	2.6E+6
	TS	N	B	23.9	12.0E+9	2.0	879.0E+3	1.8E+6	2.6E+6
	CP	S	C	17.9	4.4E+9	2.1	767.2E+3	1.6E+6	2.5E+6
	CP	N	C	17.9	4.4E+9	2.1	767.2E+3	1.6E+6	2.5E+6
S10	TS	S	B	24.0	12.0E+9	2.0	868.1E+3	1.7E+6	2.6E+6
	TS	N	B	24.0	12.0E+9	2.0	868.1E+3	1.7E+6	2.6E+6
	CP	S	C	18.0	4.4E+9	2.1	754.5E+3	1.6E+6	2.4E+6
	CP	N	C	18.0	4.4E+9	2.1	754.5E+3	1.6E+6	2.4E+6
S11	TS	S	B	18.7	12.0E+9	2.0	1.8E+6	3.7E+6	5.5E+6
	TS	N	B	18.7	12.0E+9	2.0	1.8E+6	3.7E+6	5.5E+6
	CP	S	C	14.0	4.4E+9	2.1	1.6E+6	3.4E+6	5.1E+6
	CP	N	C	14.0	4.4E+9	2.1	1.6E+6	3.4E+6	5.1E+6
S12	TS	S	B	19.2	12.0E+9	2.0	1.7E+6	3.4E+6	5.1E+6
	TS	N	B	19.2	12.0E+9	2.0	1.7E+6	3.4E+6	5.1E+6
	CP	S	C	14.4	4.4E+9	2.1	1.5E+6	3.1E+6	4.7E+6
	CP	N	C	14.4	4.4E+9	2.1	1.5E+6	3.1E+6	4.7E+6
S13	TS	S	B	23.0	12.0E+9	2.0	986.3E+3	2.0E+6	3.0E+6
	TS	N	B	23.0	12.0E+9	2.0	986.3E+3	2.0E+6	3.0E+6
	CP	S	C	18.0	4.4E+9	2.1	754.5E+3	1.6E+6	2.4E+6
	CP	N	C	18.0	4.4E+9	2.1	754.5E+3	1.6E+6	2.4E+6
S14	TS	S	B	24.0	12.0E+9	2.0	868.1E+3	1.7E+6	2.6E+6
	TS	N	B	24.0	12.0E+9	2.0	868.1E+3	1.7E+6	2.6E+6
	CP	S	C	19.0	4.4E+9	2.1	641.5E+3	1.3E+6	2.1E+6
	CP	N	C	19.0	4.4E+9	2.1	641.5E+3	1.3E+6	2.1E+6

FIGURES

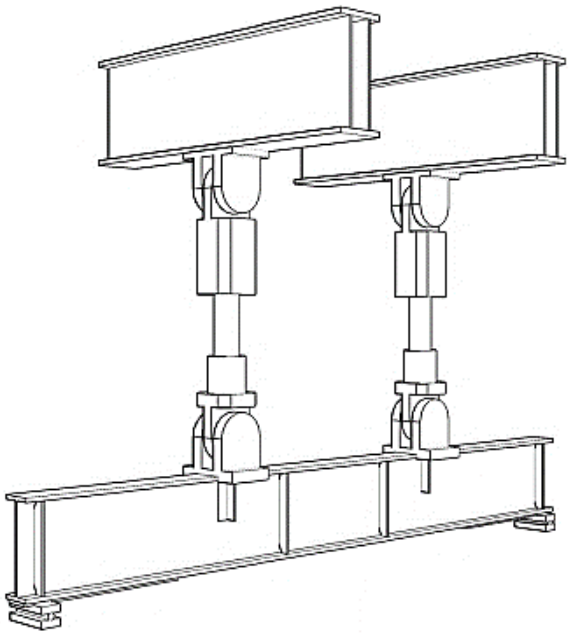

Figure 3.1: Specimen with Two Hydraulic Actuators

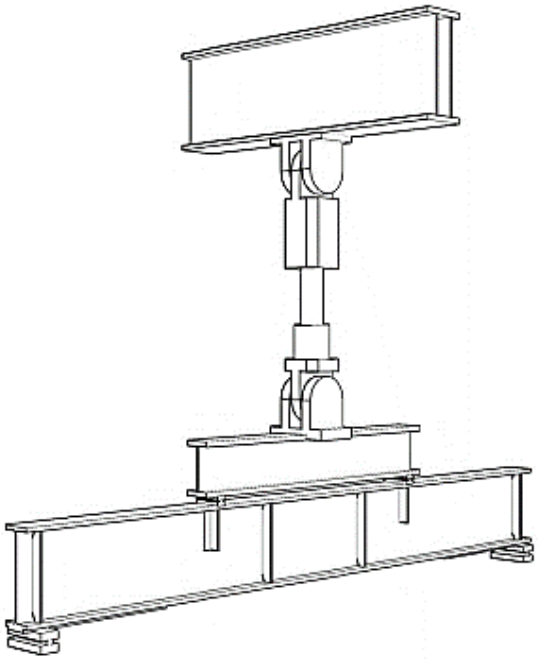

Figure 3.2: Specimen with 1 Hydraulic Actuator and Spreader Beam

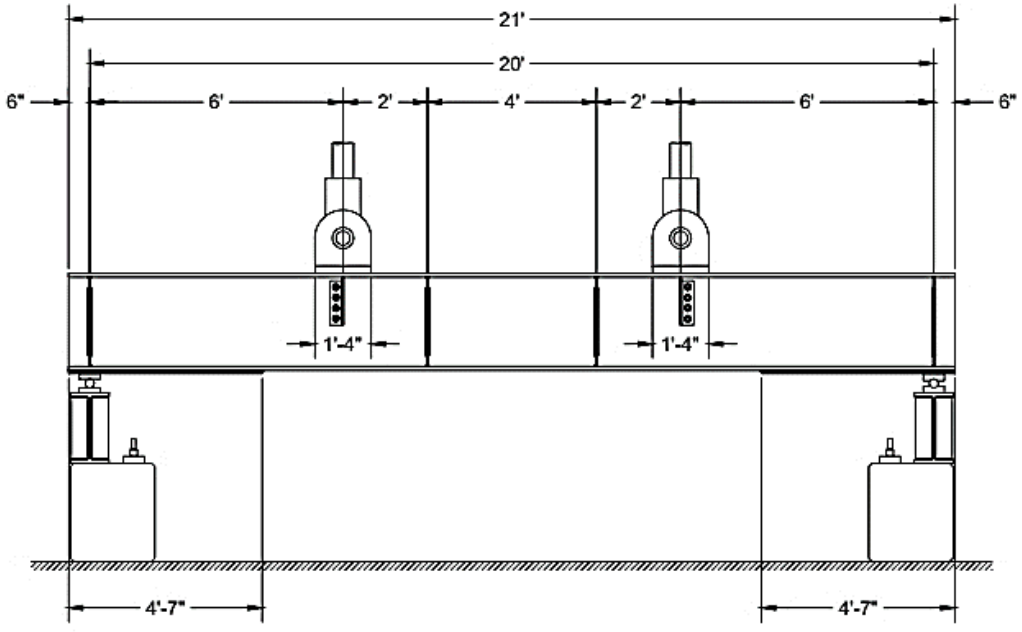

Figure 3.3: Specimen 7 with Two Actuators

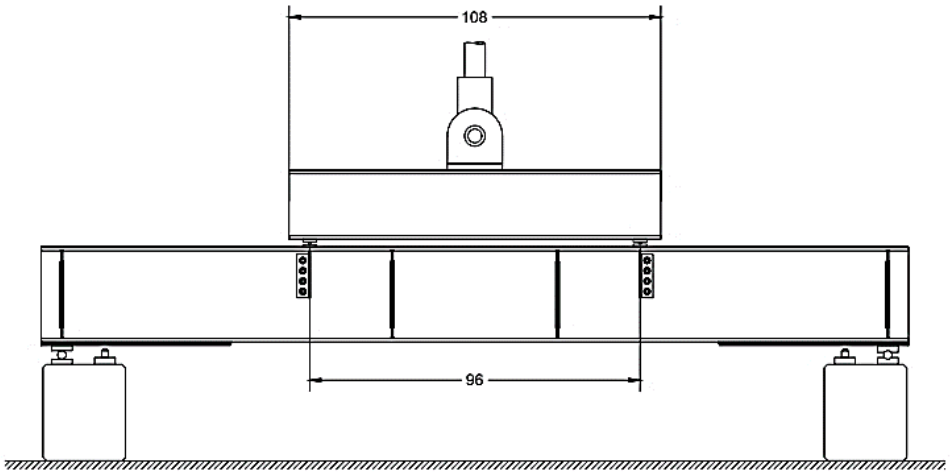

Figure 3.4: Specimen 5 with One Actuator

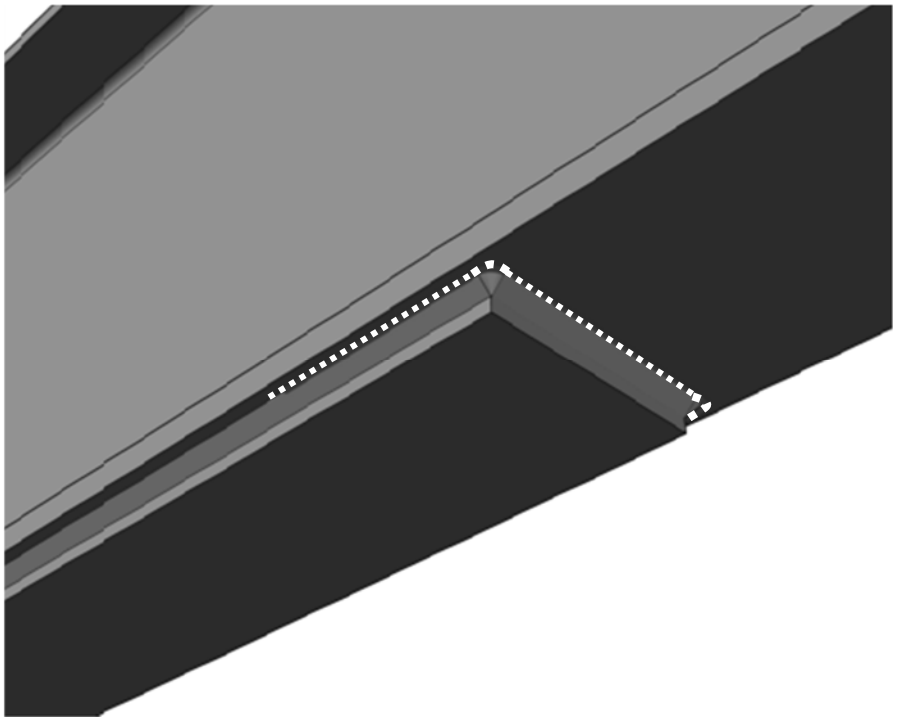

Figure 3.5: Treatment Region at Cover Plate Termination Test Detail

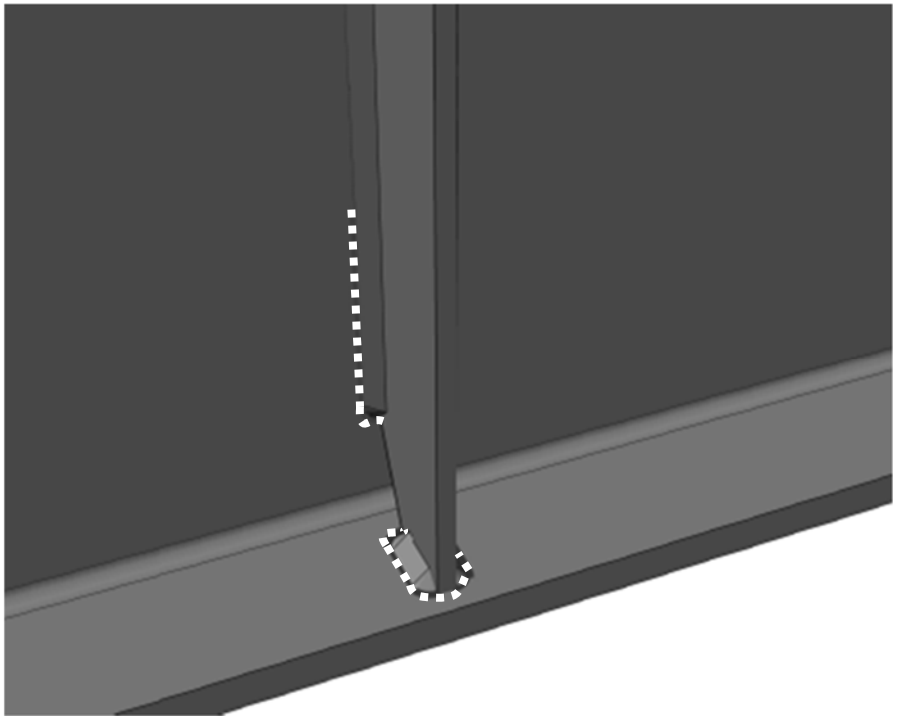

Figure 3.6: Treatment Region at Transverse Stiffener Test Detail

Figure 3.7: Application of UIT at Transverse Stiffener

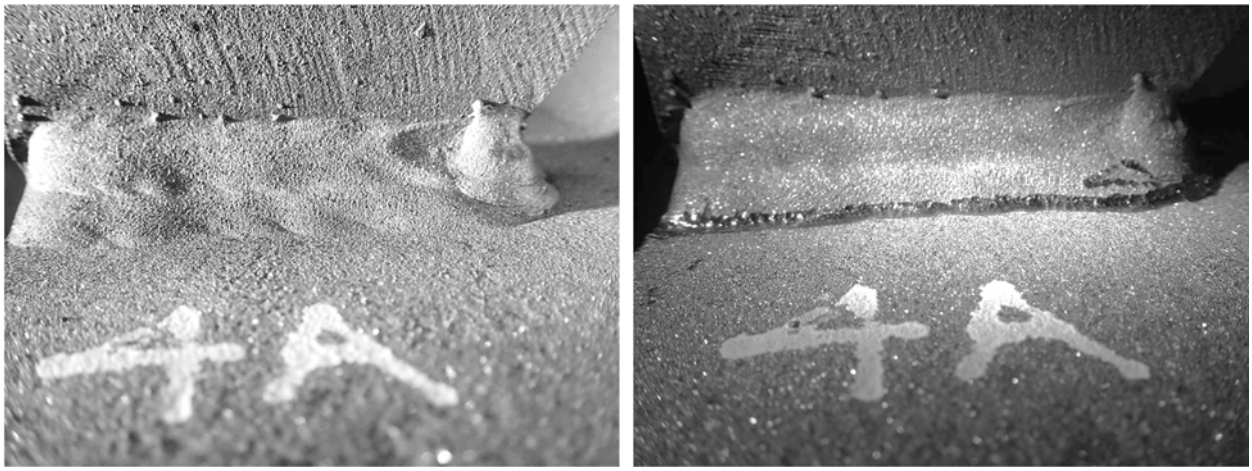

Figure 3.8a, Figure 3.8b: Transverse Stiffener Fillet Weld Toe Before and After UIT

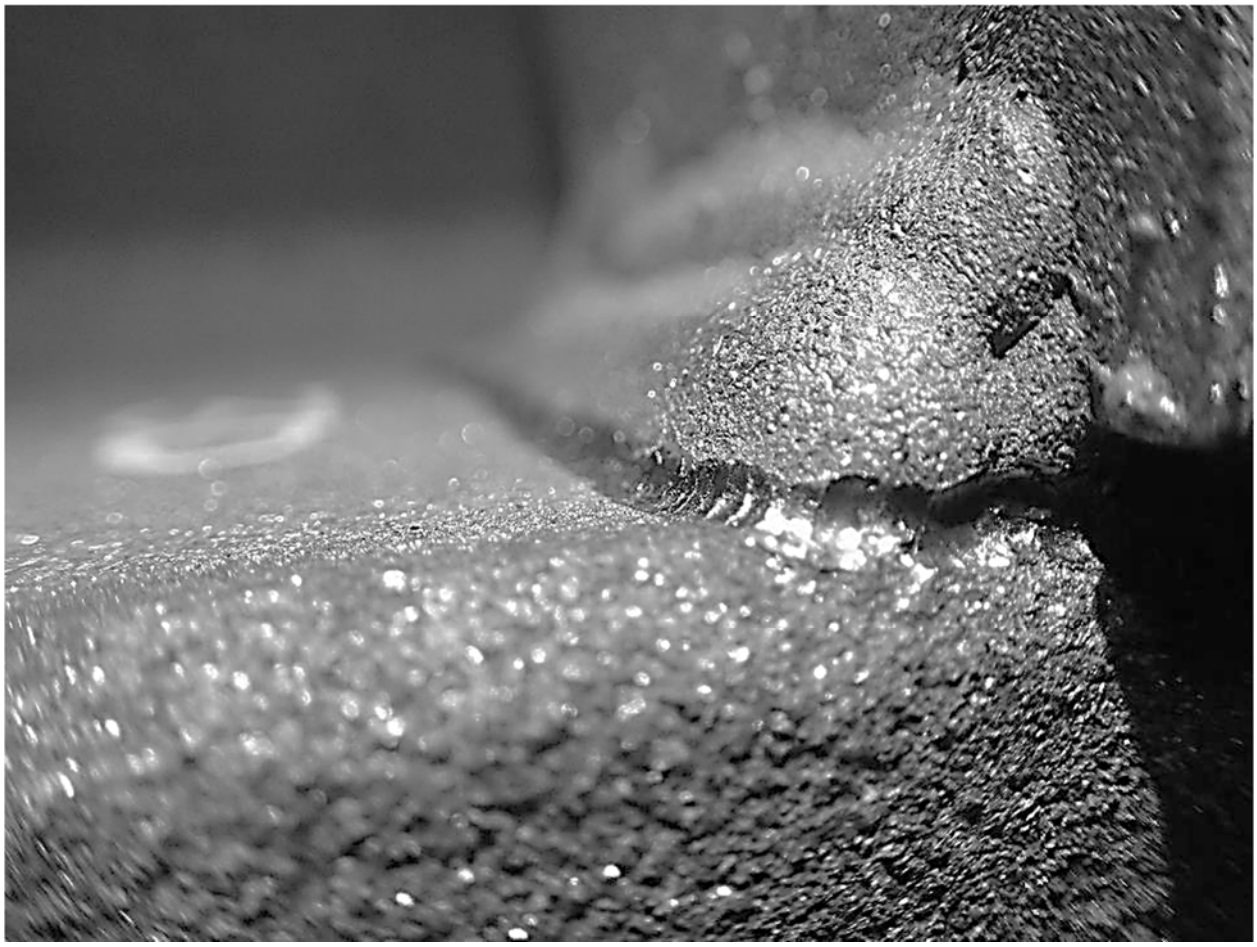

Figure 3.9: Profile of Transverse Stiffener Weld Toe After UIT

Figure 3.10a, Figure 3.10b: Cover Plate Fillet Weld Toe Before and After UIT

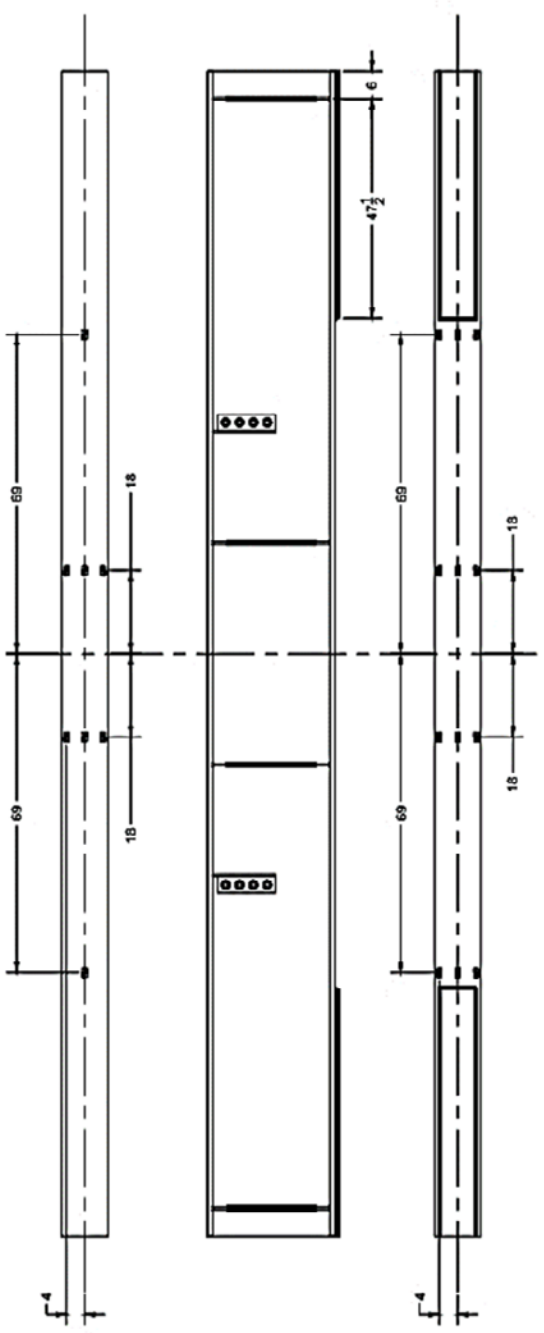

Figure 3.11: Specimen 1 – 6 Strain Gage Layout

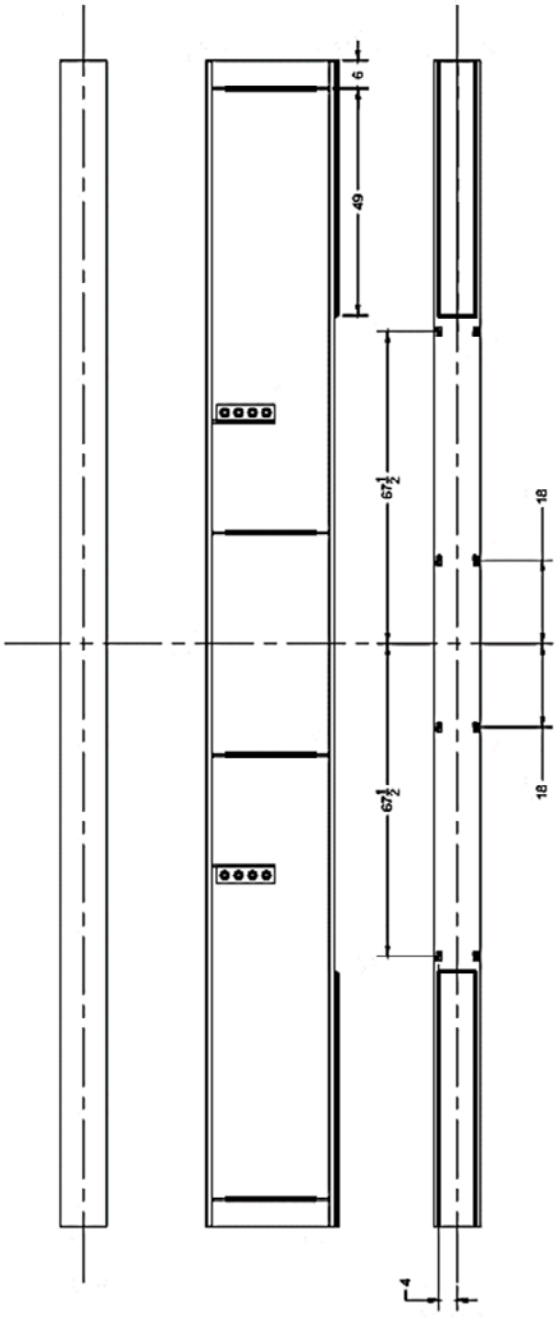

Figure 3.12: Specimen 7 – 14 Strain Gage Layout

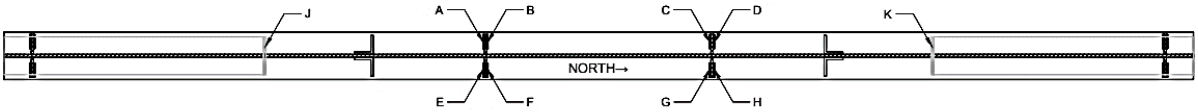

Figure 3.13: Test Detail Nomenclature

Figure 3.14: Open and Bolted Crack Arrest Holes at a Failed Cover Plate

Figure 4.1: Fatigue Crack Initiated from Transverse Stiffener Weld Toe

Figure 4.2: Fatigue Crack Initiated from as-welded Cover Plate Weld Toe

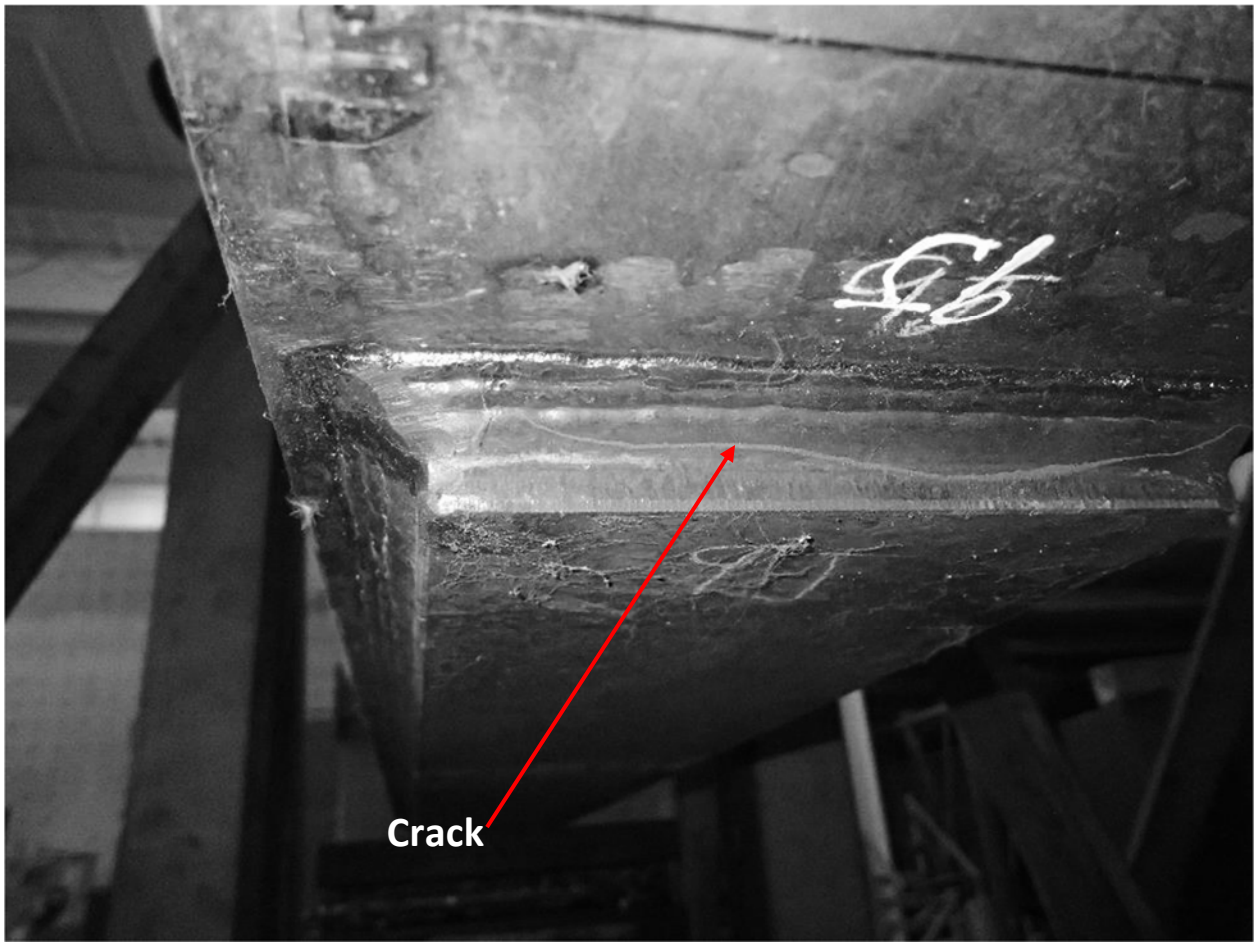

Figure 4.3a: Fatigue Crack through Weld Throat of Treated Cover Plate Weld

Figure 4.3b: Fatigue Crack through Weld Toe of Treated Cover Plate Weld

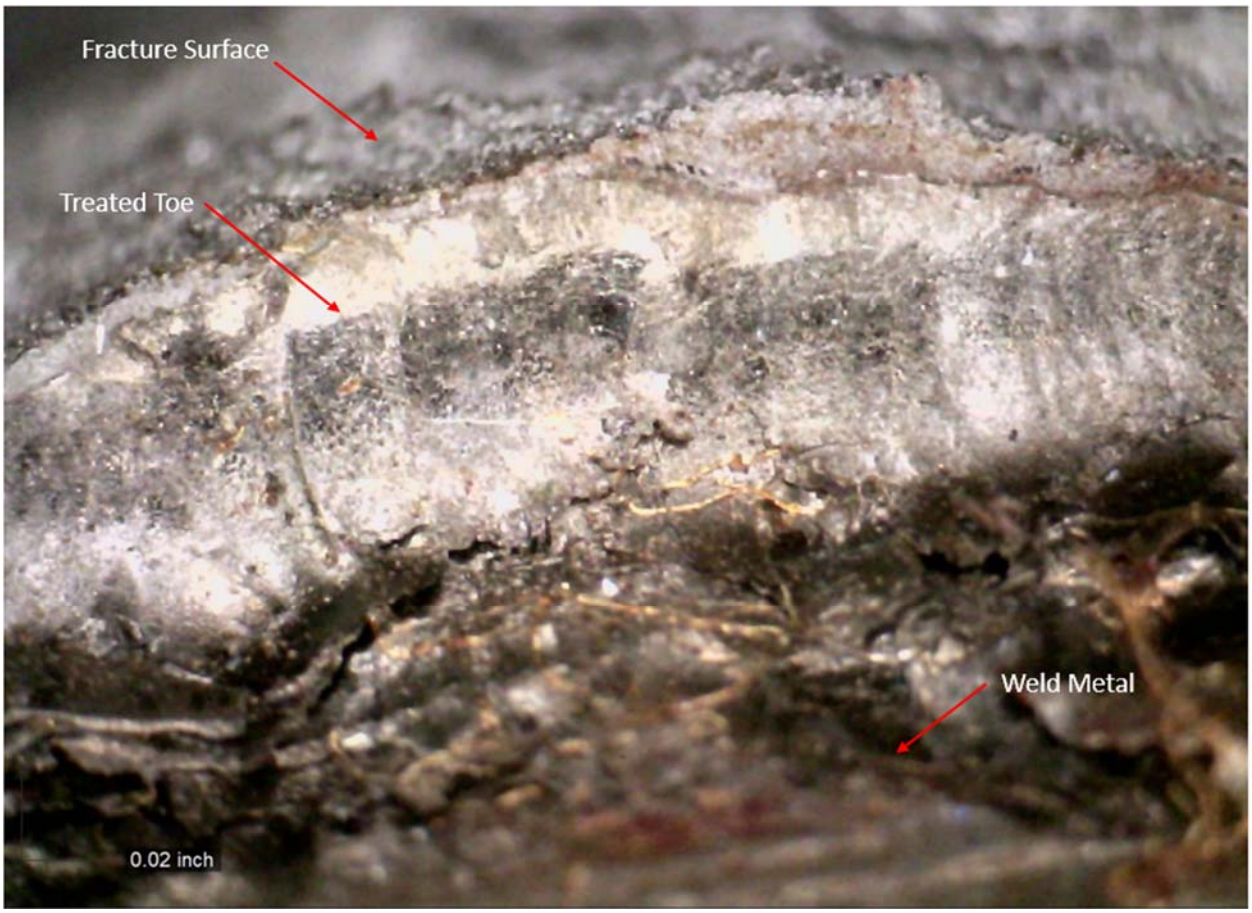

Figure 4.3c: Effective Treatment Application

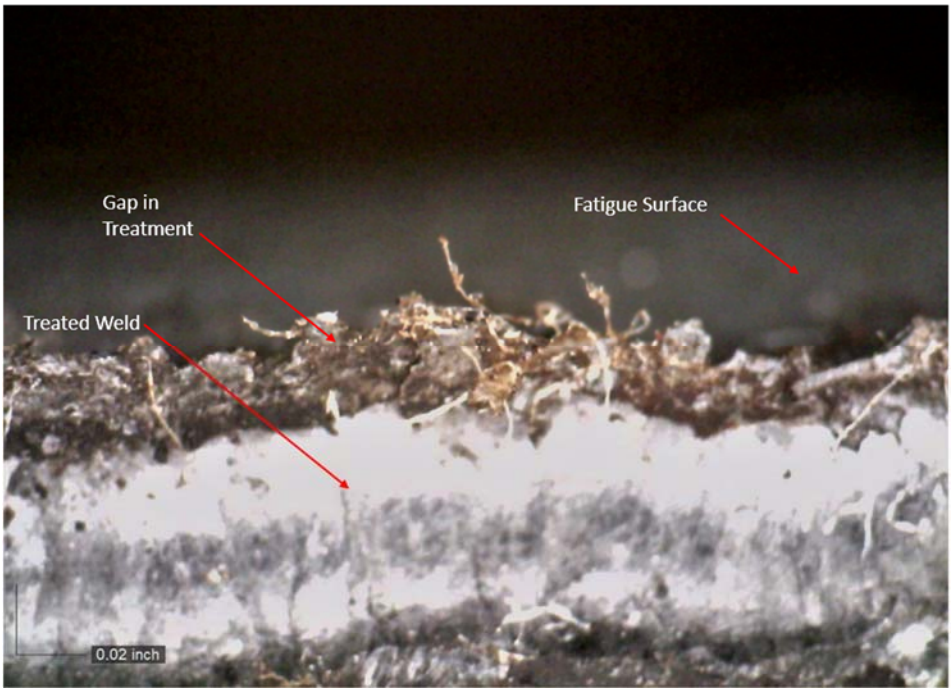

Figure 4.3d: Gap in Treatment Application

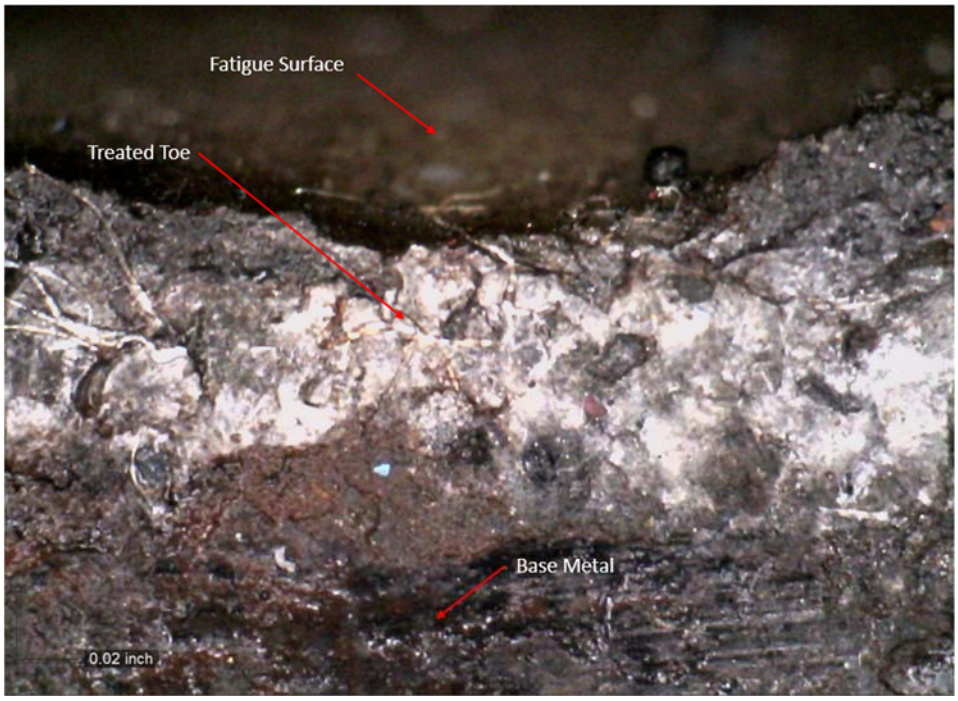

Figure 4.3e: Gap in Treatment Application

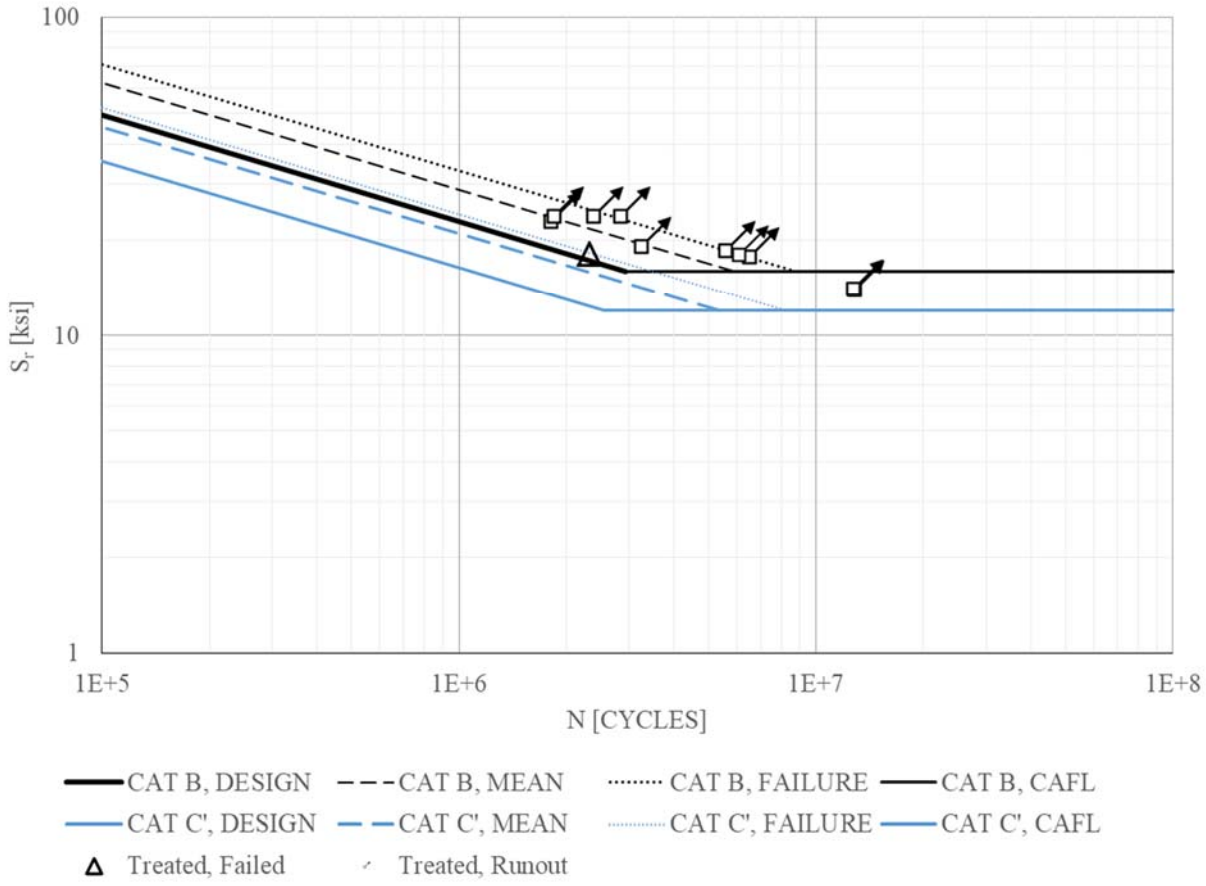

Figure 4.4: S-N Diagram, Treated Transverse Stiffeners

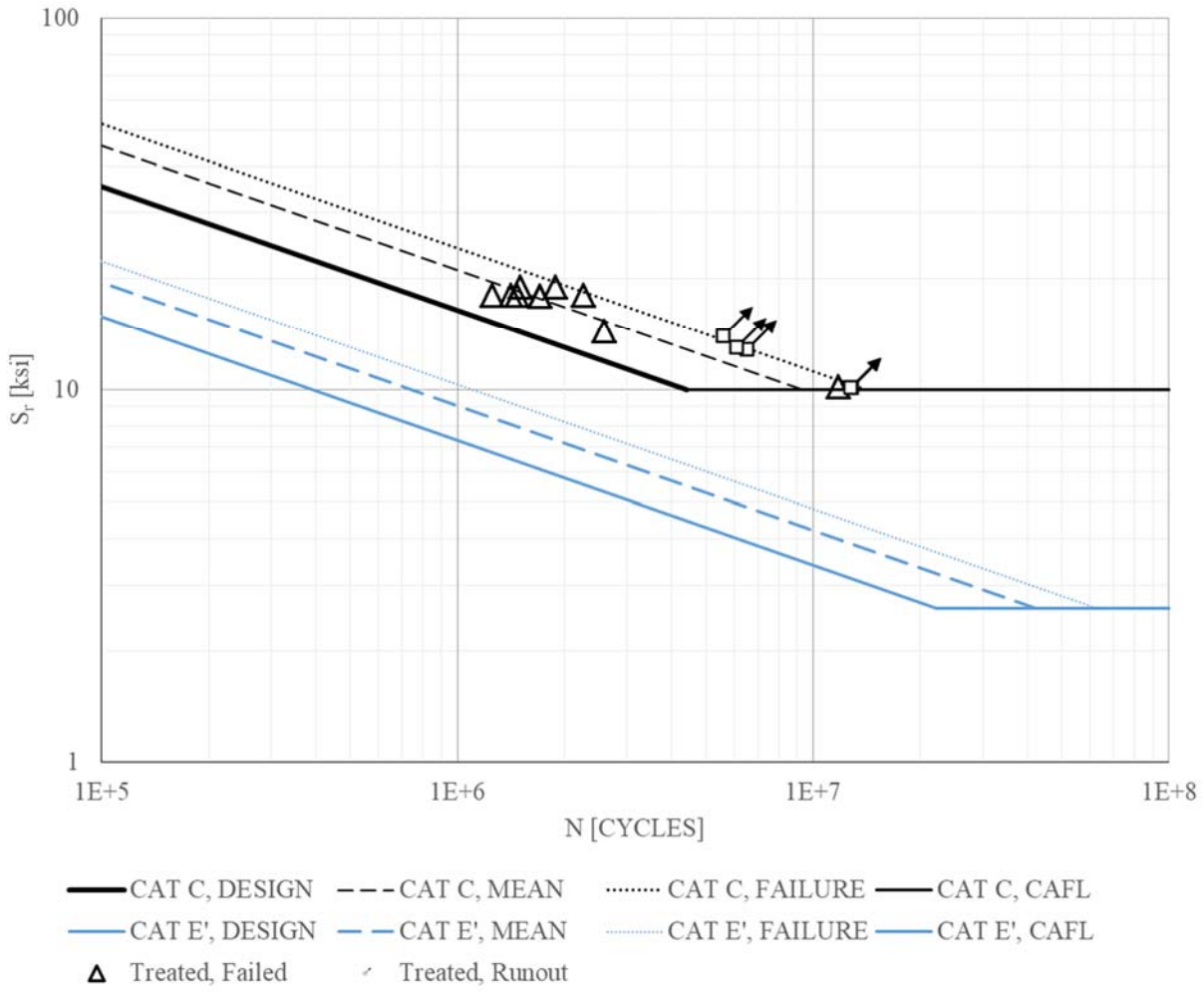

Figure 4.5: S-N Diagram, Treated Cover Plates

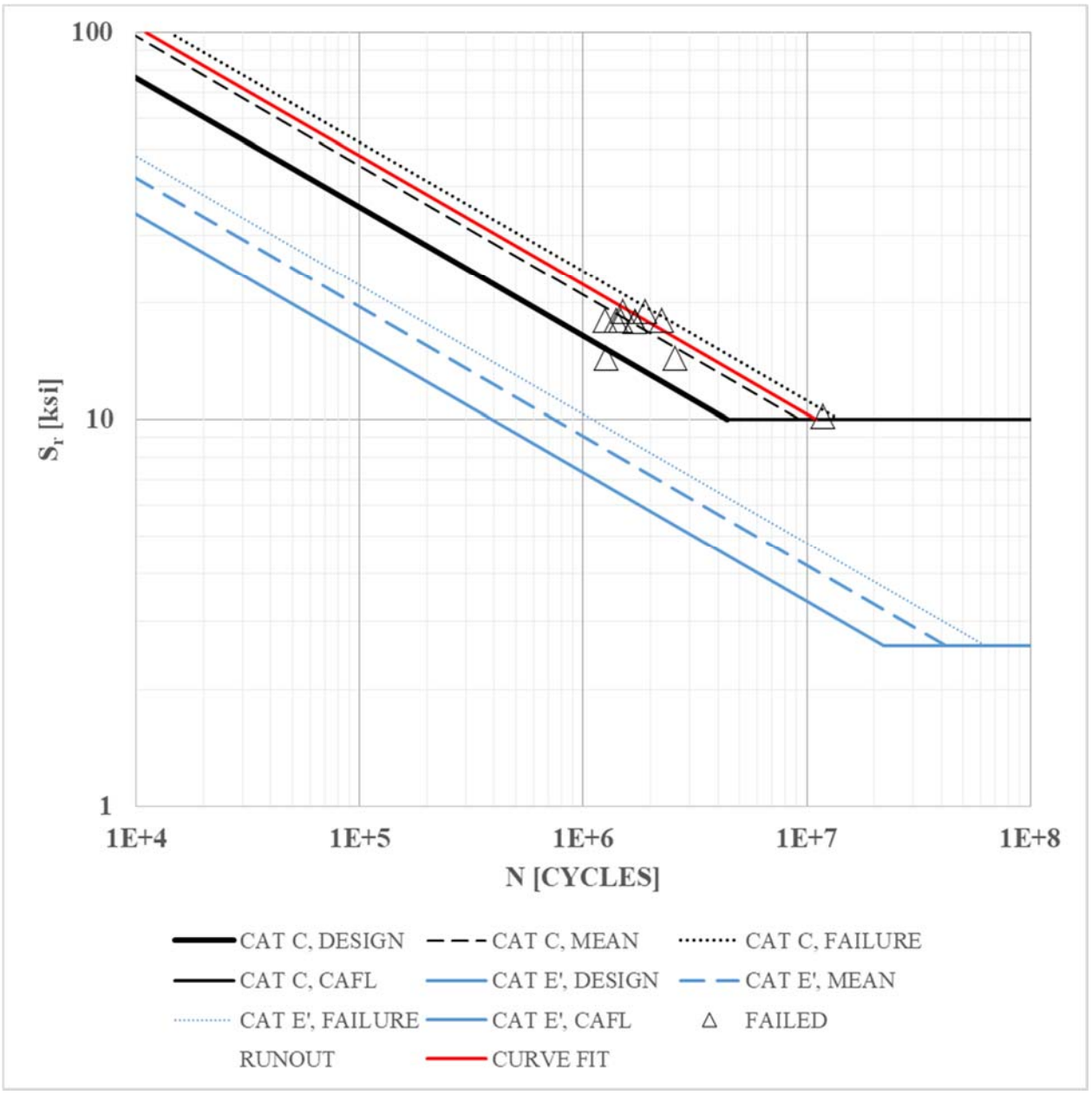

Figure 4.6: S-N Diagram, Weld Root Failures of Treated Cover Plates with Curve Fit

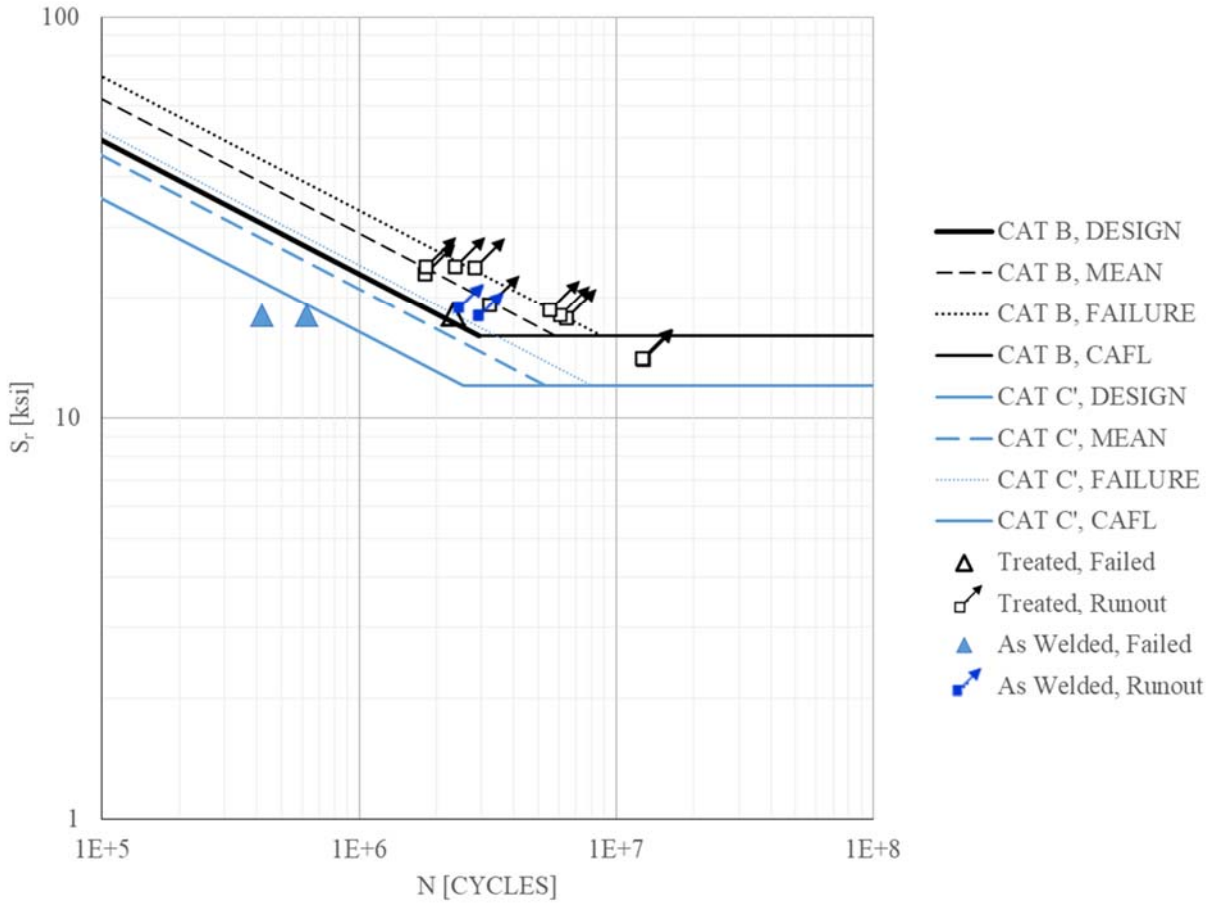

Figure 4.7a: S-N Diagram, All Transverse Stiffener Details

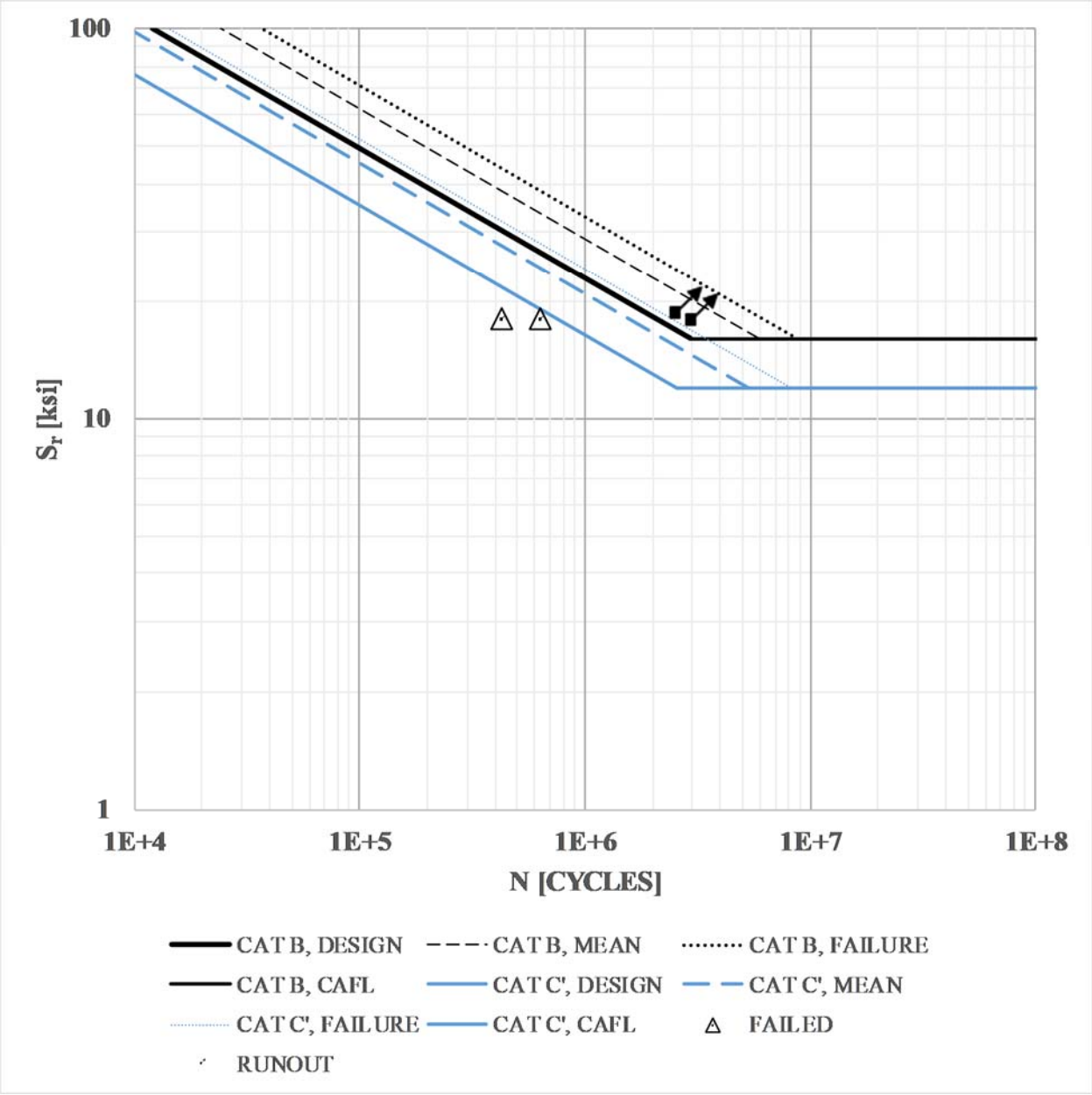

Figure 4.7: S-N Diagram, Untreated Transverse Stiffeners

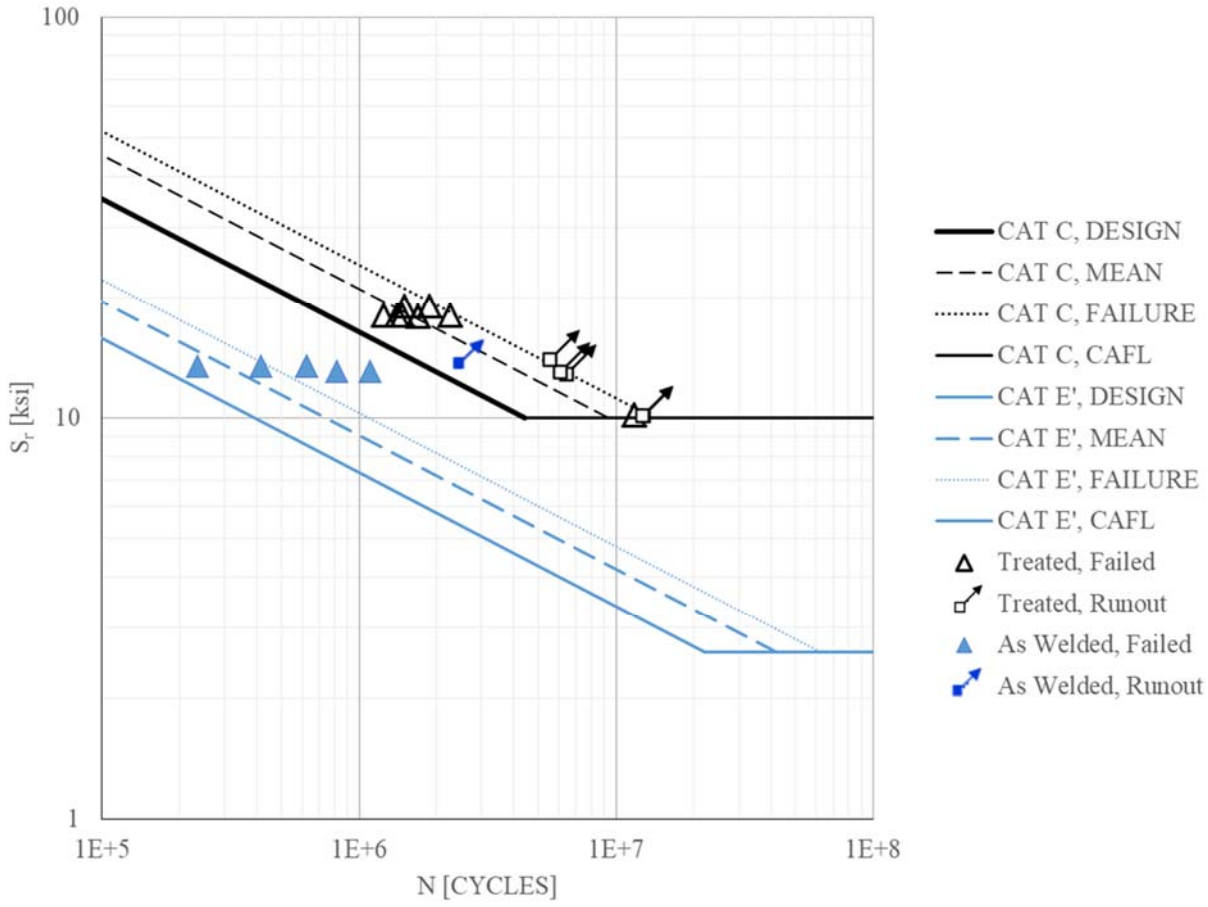

Figure 4.8a: S-N Diagram, All Cover Plate Details

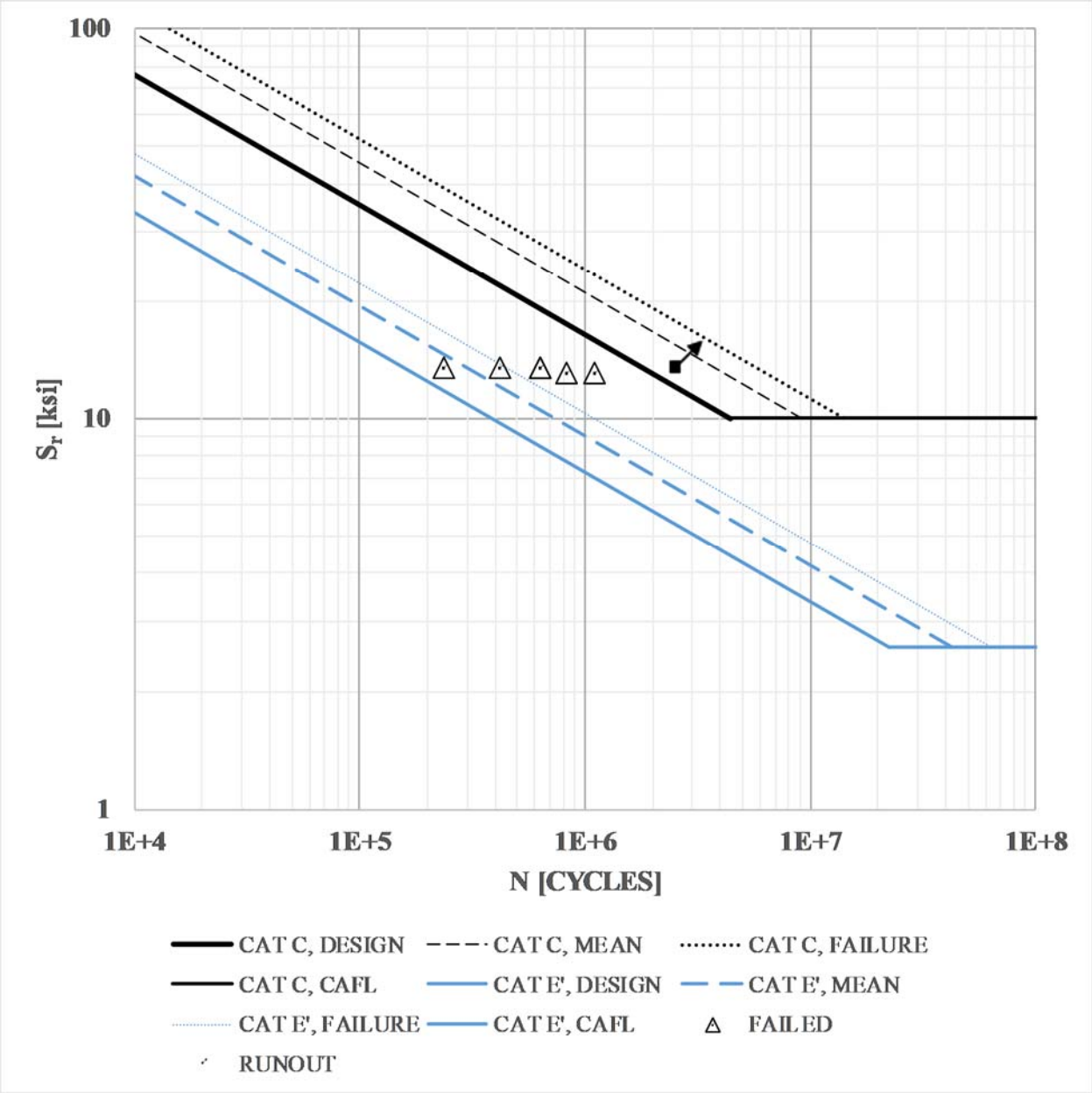

Figure 4.8b: S-N Diagram, Untreated Cover Plates

REFERENCES

American Association of State Highway and Transportation Officials. (2008). AASHTO LRFD Bridge Construction Specifications, Second Edition, 2008 Interim Revisions.

American Association of State Highway and Transportation Officials. (2014). AASHTO LRFD Bridge Design Specifications, Seventh Edition, 2014 US Customary Units.

Bowman, M., Fu, G., Zhou, E., Connor, R., Godbole, A. (2012). Fatigue Evaluation of Steel Bridges. Retrieved from http://nap.edu/22774

Cheng, X., Yen, B., Fisher, J. (2012, April 26). Fatigue Resistance Enhancement and Residual Stress Modification of Welded Steel Structures by Various Post-Weld Treatments. Retrieved from https://doi.org/10.1061/41016(314)4

Delaware Department of Transportation (2015). Bridge Design Manual. Retrieved from https://www.deldot.gov/Publications/manuals/bridge_design/pdfs/2015/bridge_design_manual.pdf

Dexter, R., Ocel, J. (2013, March). Manual for Repair and Retrofit of Fatigue Cracks in Steel Bridges. Retrieved from https://www.fhwa.dot.gov/bridge/steel/pubs/hif13020/hif13020.pdf

Fish, P., Schroeder, C., Connor, R. J., & Sauser, P. (2015). Fatigue and Fracture Library for the Inspection, Evaluation, and Repair of Vehicular Steel Bridges. Purdue University. West Lafayette, Indiana. Available from: http://dx.doi.org/10.5703/1288284315520

Fisher, J., Frank, K., Hirt, M., McNamee, B. (1969, September). Effect of Weldments on the Fatigue Strength of Steel Beams. Retrieved from https://preserve.lehigh.edu/cgi/viewcontent.cgi?article=1322&context=engr-civil-environmental-fritz-lab-reports

Fisher, J., Albrecht, P., Yen, B., Klingerman, D., McNamee, B. (1974). NCHRP Report 147, Fatigue Strength of Steel Beams with Welded Stiffeners and Attachments. Retrieved from http://onlinepubs.trb.org/Onlinepubs/nchrp/nchrp_rpt_147.pdf

Fisher, J., Hausammann, H., Pense, A. (1979, January). Retrofitting procedures for fatigue damaged full scale welded bridge beams. Retrieved from http://preserve.lehigh.edu/engr-civil-environmental-fritz-lab-reports/2191

Gunther, H., Kuhlmann, U., Durr, A. (2005, January). Rehabilitation of Welded Joints by Ultrasonic Impact Treatment (UIT). Retrieved from https://www.researchgate.net/publication/233660768_Rehabilitation_of_Welded_Joints_by_Ultrasonic_Impact_Treatment_UIT

Indiana Department of Transportation. (2012, March 1). 711-B-190 PEENING WELDS BY MEANS OF ULTRASONIC IMPACT TREATMENT. Retrieved from http://www.in.gov/dot/div/contracts/standards/rsp/sep11/700/711-B-190%20120301.pdf

New York Department of Transportation. (2016, June). ITEM 586.30010016 – ULTRASONIC IMPACT TREATMENT ON COVER PLATE TRANSVERSE END WELDS. Retrieved from https://www.dot.ny.gov/spec-repository-us/586.30010016.pdf

Palmatier, A. (2005, May). Ultrasonic Impact Treatment of Traffic Signal Mast Arm Welds. Retrieved from https://fsel.engr.utexas.edu/pdfs/Thesis4.pdf

Roy, S., & Fisher, J. (2006). Experimental and Analytical Evaluation of Enhancement in Fatigue Resistance of Welded Details Subjected to Post-Weld Ultrasonic Impact Treatment, ProQuest Dissertations and Theses.

Roy, S., & Fisher J., (2003, September). Fatigue resistance of welded details enhanced by ultrasonic impact treatment (UIT). Retrieved from https://doi.org/10.1016/S0142-1123(03)00151-8

Takamori, H., Fisher, J. (2000, March 3). Tests of Large Girders Treated to Enhance Fatigue Strength. Retrieved from https://doi.org/10.3141/1696-12

Takamori, H., & Fisher, J. (2000). Improving Fatigue Strength of Welded Joints, ProQuest Dissertations and Theses.

Texas Department of Transportation. (2004). SPECIAL SPECIFICATION 7084 Ultrasonic Impact Treatment. Retrieved from http://ftp.dot.state.tx.us/pub/txdot-info/cmd/cserve/specs/2004/spec/ss7084.pdf

Virginia Department of Transportation. (2016). Road and Bridge Specifications. Retrieved from http://www.virginiadot.org/business/resources/const/VDOT_2016_RB_Specs.pdf

APPENDIX I

The following are proposed changes to the AASHTO LRFD Bridge Construction Specifications.

11.9 Ultrasonic Impact Treatment (UIT)

11.9.1 General

C11.9.1

Typical post-weld treatment includes ultrasonic impact treatment, heat treatment, grinding, weld toe remelting (GTAW dressing or plasma arc dressing), hammer peening, and shot peening.

~~Based on research performed at Lehigh University, the fatigue strength of welded connections can be improved by post weld Ultrasonic Impact Treatment (S. Roy, et al., 2005; S. Roy, and J.W. Fisher, 2005).~~ Research performed at Lehigh University showed that fatigue strength of welded connections can be improved by post-weld 27 kHz Ultrasonic Impact Treatment (S.Roy, et al., 2005; S. Roy and J.W. Fisher, 2005). Subsequent research performed at Purdue University showed post-weld 20 kHz Ultrasonic Impact Treatment has equivalent effectiveness (R. Connor, J. Lloyd, and J. Hui, 2017). In general, the objective of UIT is to plastically deform the material at the weld toes and introduce residual compressive stresses substantially greater than the largest anticipated tensile stresses to a depth of no less than 0.02 in. (0.5 mm).

Treatment is necessary only at the weld toe. The weld toe is defined as the interface of the weld metal and base metal. Due to the finite size of the UIT needles and the recommended treatment procedure, some base metal adjacent to the weld toe will get treated.

~~To successfully accomplish the treatment, the following sample procedure should be included in the special provisions of the contract documents, unless otherwise recommended by the UIT equipment Manufacturer:~~ The following is a sample procedure for a particular 27 kHz Ultrasonic Impact Treatment system. Due to the proprietary nature of UIT, operating parameters may vary depending on equipment manufacturer. Whether a 20 kHz or 27 kHz system is selected, the treatment should be carried out following the equipment manufacturer's recommended practices.

		[No proposed changes to remainder of C11.9.1]
11.9.2 Procedure UIT shall be accomplished in accordance with the equipment Manufacturer's recommendations, except as specifically described in the contract documents. The use of UIT shall be limited to base metal with a specified minimum yield strength of 100 ksi (690 MPa) or less. Prior to UIT, the weld toe to receive UIT shall be visually inspected and magnetic particle-tested for conformance to the quality standards specified in the contract documents. ~~The instrument shall be calibrated against the maximum flaw size allowed.~~ ~~—~~Discontinuities greater than 1/32 in. (0.79 mm) shall be repaired satisfactorily prior to initiating the work. UIT shall be done along the toe of the weld in a manner that will cause the center of the resultant treatment groove to be at the weld toe, with equal treatment and smooth transition to the adjacent weld and base metal. UIT shall be performed so as to result in a uniform groove with a distinct and uniform bright metallic surface, as verified by visual inspection immediately after completion. When viewed under a 10x magnifying glass, the groove shall be free from any visible indications of the untreated base metal or weld metal. If such untreated indications exist within the treated area, such area shall be retreated to obtain a uniform, bright metallic surface across the entire surface of the UIT groove. *[No proposed changes to remainder of 11.9]*		<u>To ensure that a weld where a crack has initiated is not treated, the weld toe is to be inspected using some form of reliable NDT technique. Visual inspection and magnetic particle testing is recommended. While the term "discontinuity" is very general term, the inspection should be focused on those that are crack like and less than 1/32 in. in length as the subsurface depth cannot be measured.</u>